MATHEMATICS RESEARCH CENTER, UNITED STATES ARMY
THE UNIVERSITY OF WISCONSIN

Contract No.: DA-31-124-ARO-D-462

NUMERICAL INTEGRATION OF THE NAVIER-STOKES EQUATIONS IN TWO DIMENSIONS

S. C. R. Dennis and Gau-Zu Chang

MRC Technical Summary Report #859
July 1969

Madison, Wisconsin

ABSTRACT

In this report, a method of numerical integration of the Navier-Stokes equations for two-dimensional flows is described. Both steady and time-dependent flows are considered. The method is restricted to classes of motion defined in a rectangular domain, but by the use of a suitable transformation this includes a large class of problems describing the flow past cylinders in an otherwise unbounded fluid. The formulation of the problem in terms of the stream function and vorticity is adopted.

Numerical illustrations of the method include results for steady flow past a circular cylinder for Reynolds numbers, based on the diameter, up to 100. The problem of symmetrical flow past an elliptic cylinder with the major axis in the direction of undisturbed flow is also investigated for a range of Reynolds numbers, based on the length of the major axis, from 1 to 200. The ratio of the major to the minor axis is taken as 5 to 1. Some of the numerical results were computed on the CDC 3600 at the University of Wisconsin and some on the IBM 7040 at the University of Western Ontario.

The present report is a modified and extended version of a paper presented to the U.S. Army Numerical Analysis Conference, Fort Monmouth, New Jersey, April 25 - 26, 1968. The numerical results for flow past a circular cylinder given in the previous paper have been improved by more elaborate calculations.

NUMERICAL INTEGRATION OF THE NAVIER-STOKES EQUATIONS IN TWO DIMENSIONS

S.C.R. Dennis and Gau-Zu Chang

INTRODUCTION

The problem of integrating the Navier-Stokes equations by numerical methods has been of interest for some time. Recently, much attention has been concentrated on studies of time-dependent flows. One reason is that, starting from some initial state, if a stable integration procedure is chosen and the integrations carried on for sufficiently long time, a steady-state solution may be approached. Another is that time-dependent integrations may be used to predict flow configurations which are basically unsteady for all values of the time, no matter how large. In this report we shall start by considering the time-dependent problem. The work is then extended to the case of steady flows.

If incompressibility of the fluid is assumed, the Navier-Stokes equations can be written in the usual dimensionless form

$$\partial \underset{\sim}{V}/\partial t + (\underset{\sim}{V}\cdot\nabla)\underset{\sim}{V} = -\text{grad } p + R^{-1}\nabla^2\underset{\sim}{V}, \qquad (1)$$

where $\underset{\sim}{V}$ and p are, respectively, the dimensionless velocity vector and the pressure, t is the time, and R is a generalized Reynolds number based on some typical length and typical velocity in the flow field. Definitions of these quantities in terms of dimensional quantities are given in the Appendix. For two-dimensional flow in the (x,y)-plane, the equation of continuity div $\underset{\sim}{V}$ = 0 can be satisfied by introducing the dimensionless stream function $\psi(x,y,t)$, related to the velocity components (u,v)

Sponsored in part by the Mathematics Research Center, United States Army, Madison, Wisconsin, under Contract No.: DA-31-124-ARO-D-462 and in part by the National Research Council of Canada.

by the equations

$$u(x,y,t) = \partial\psi/\partial y,\ v(x,y,t) = -\partial\psi/\partial x. \tag{2}$$

Also, the equation which results from eliminating the pressure from (1) can be expressed in terms of the negative dimensionless scalar vorticity $\zeta(x,y,t)$, defined by $\zeta = \partial u/\partial y - \partial v/\partial x$. Thus it is found that the equations governing these two quantities are

$$\nabla^2\psi = \zeta, \tag{3}$$

$$\frac{\partial\zeta}{\partial t} + \frac{\partial\psi}{\partial y}\frac{\partial\zeta}{\partial x} - \frac{\partial\psi}{\partial x}\frac{\partial\zeta}{\partial y} = R^{-1}\nabla^2\zeta, \tag{4}$$

where $\nabla^2 = \partial^2/\partial x^2 + \partial^2/\partial y^2$. The necessary boundary conditions are as follows. Where the fluid is in contact with a solid boundary designated by the curve C,

$$\psi \text{ and } \partial\psi/\partial n \text{ are known on C}, \tag{5}$$

where $\partial/\partial n$ is differentiation normal to C. If the flow is enclosed, as in the case of motion in a closed cell, these are the only conditions. If it is open, as in the case of flow past a cylinder in an unbounded fluid, conditions at infinity must be imposed. Generally these reduce to the fact that the asymptotic behavior of both ψ and ζ is known as infinity is approached. However, the important point in both problems is that two conditions are prescribed for ψ on C and none for ζ.

This latter feature could tend to make the integration procedure slower than it might otherwise be. The solution of the Poisson-type equation (3) is a boundary-value problem for a given step in time and has to be solved by boundary-value techniques, which are sometimes slow if iterative methods are used. The solution of equation (4) on the other hand, is a marching (or step-by-step) problem in time. An integration of the pair of equations proceeeds as follows. To fix ideas consider

flow past a cylinder, in which the domain of the solution is a region D between a closed contour C on which the conditions (5) hold and an outer contour C_1, on which boundary conditions for both ζ and ψ may be supposed known. Suppose at a given time t, both ζ and ψ are known at all points of a finite-difference grid covering D and also at all necessary points of C and C_1. Then the integration through time $t + \Delta t$ consists of the successive operations:

(i) By forward integration of equation (4), $\zeta(x,y,t + \Delta t)$ is determined from $\zeta(x,y,t)$ at all grid points in D and on C_1, but not on C since no boundary condition for ζ is known there.

(ii) From $\zeta(x,y,t + \Delta t)$ at grid points within D, $\psi(x,y,t + \Delta t)$ is determined from equation (3) as a boundary-value problem with ψ known on C and C_1.

(iii) The (as yet unused) condition for $\partial\psi/\partial n$ on C is used to calculate $\zeta(x,y,t + \Delta t)$ on C from computed values of $\psi(x,y,t + \Delta t)$ at grid points in the neighborhood of C. The solution at time $t + \Delta t$ is thus completed everywhere. Successive applications of the whole process determine the solution at any subsequent time.

In the present report the solution of the boundary-value problem in step (ii) of the above procedure is modified in certain classes of problem defined in rectangular domains. Flow past a cylinder falls into such a class, for by a suitable conformal transformation the domain of the two-dimensional flow past cylinders of various shapes can be mapped onto a semi-infinite rectangle. It is shown that for this problem we can replace the boundary-value problem in step (ii) of the above procedure by a step-by-step integration which determines the

stream function by direct methods. In fact, equation (3) is solved as a step-by-step problem in a single space variable.

The basis of the method for flow past cylinders is the following. Suppose step (i) of the above procedure has been carried out. It is shown that certain necessary conditions involving integrals of $\zeta(x,y,t + \Delta t)$ evaluated throughout the region D must at this stage be satisfied. The satisfaction of these conditions allows $\zeta(x,y,t + \Delta t)$ to be determined on the boundary C entirely from the internal solution for $\zeta(x,y,t + \Delta t)$ and without any determination of the internal solution for $\psi(x,y,t + \Delta t)$. The solution for $\zeta(x,y,t + \Delta t)$ is then complete. Since this function is now known on C as well as in D, it is now possible to integrate equation (3) subject to the conditions (5) by a step-by-step procedure in space, since sufficient boundary conditions are given on C. This procedure determines $\psi(x,y,t + \Delta t)$ on C_1 as part of the solution and this must come out in accordance with the known boundary condition for ψ on C_1, giving an adequate check on the procedure. The method is useful in this type of problem because the precise boundary condition for ψ on C_1 at a given time is not an easy one to specify.

Although most attention is given to the problem of flow past a cylinder, the method is not restricted to this problem. As an illustration another type of problem, that of flow in a closed rectangular cell, is considered. The method is less satisfactory here although the same objective, construction of a step-by-step integration of equation (3), is achieved. In both classes of problems the procedure is based on the reduction of equation (3) to a set of ordinary differential equations in one space variable. This is done by standard

Fourier analysis. The resulting ordinary differential equations are then solved by step-by-step methods. For flow past cylinders the range of integration is, in theory, infinite. In the closed cell problem it is finite. In both cases a special technique is used for solving these differential equations. It is explained and illustrated by a numerical example over a finite range of integration.

The method is subsequently extended to the equations of steady motion. Here, $\partial\zeta/\partial t = 0$ in equation (4) and the resulting equation is solved as a boundary-value problem of Dirichlet type along with the equation (3). The pair of equations (3) and (4) are solved iteratively by a process similar to that used in the time-dependent case.

Results are given for symmetrical steady flow past a cylinder in two separate cases. For a circular cylinder, results for Re = 5, 7, 10, 20, 40, 70 and 100, where Re is the Reynolds number based on the diameter, have been obtained by solving the equations of steady motion. Results for an elliptic cylinder with its major axis in the direction of undisturbed flow and its major and minor axes in the ratio 5 to 1 have been obtained for Re = 1 to 200 by integrating the time-dependent equations for large enough times for a steady state to be reached. Here, Re is the Reynolds number based on the major axis. In neither case is Re the same as the generalized number R in (1), but it is related to it. Unfortunately, it is difficult to choose the general nondimensionalization so that R comes out exactly as desired in individual cases.

PROBLEMS CONSIDERED AND REPRESENTATION BY DIFFERENCE EQUATIONS

A typical problem of flow in a closed rectangular cavity is indicated in Figure 1. At time $t < 0$ the walls OX, XY, YZ and ZO of the cavity are at rest and there is no flow. At time $t \geq 0$ the upper wall

YZ is moved with constant velocity u = -1. All quantities are assumed to be dimensionless. The Reynolds number can be based on the actual length of one of the walls, say d, and the magnitude of the actual velocity of the upper wall U. Thus $R = Ud/\nu$, where ν is the coefficient of kinematical viscosity. The boundary C mentioned in the introduction is the boundary of the rectangle and the domain D its interior.

Boundary conditions for the stream function are obtained from the equations (2). Thus for $t < 0$, $\psi(x,y,t) = 0$ within D and on its boundary C. For $t \geq 0$ we have

$$\left.\begin{aligned} &\text{On OX: } \psi = \partial\psi/\partial y = 0 \\ &\text{On XY: } \psi = \partial\psi/\partial x = 0 \\ &\text{On YZ: } \psi = 0,\ \partial\psi/\partial y = -1 \\ &\text{On ZO: } \psi = \partial\psi/\partial x = 0. \end{aligned}\right\} \qquad (6)$$

If the solution is started from the initial state of rest it may be continued indefinitely subject to the conditions (6). For large enough time the solution will generally tend to a steady state in which all quantities are independent of time. Equations (6) give the boundary conditions for the steady problem. Solutions to the time-dependent and steady problems for various rectangles, using numerical methods, have been given in the literature. The time-dependent problem has been considered by Greenspan, Jain, Manohar, Noble and Sakurai [1]. Steady-state solutions have been given by Kawaguti [2], Simuni [3], Mills [4] and Burggraf [5]. Both types of problems have recently been considered by Zabransky [6].

For flow past cylinders a typical problem is that of a cylinder of infinite length initially at rest in an infinite, motionless, fluid.

At time $t = 0$ it starts to move, and subsequently continues to move, with constant velocity in a direction perpendicular to its axis. The fluid at large enough distances is assumed to remain undisturbed. Actually we shall adopt the following equivalent formulation. At $t < 0$, the cylinder and fluid are moving together with velocity $u = 1$ parallel to the fixed x-axis. At $t = 0$ the cylinder is brought to rest and subsequently remains at rest. The fluid at large enough distances from the cylinder is assumed to remain undisturbed with velocity $u = 1$ for all t. If C denotes the contour of the cylinder and D the infinite domain outside it then, with regard to fixed rectangular axes with origin inside C, the boundary conditions for the stream function are

$$\left.\begin{aligned} &t < 0: \ \psi = y \text{ throughout } D \\ &t \geq 0: \ \psi = \partial\psi/\partial n = 0 \text{ on } C \\ &\qquad \partial\psi/\partial y \to 1, \ \partial\psi/\partial x \to 0, \text{ as } x^2 + y^2 \to \infty. \end{aligned}\right\} \qquad (7)$$

The conditions for $t \geq 0$ are the appropriate conditions for steady flow.

We shall restrict ourselves to flows which are symmetrical about the x-axis. Thus in practice D can be limited to the region of the upper half-plane outside the upper half of C, viz. the region above GHIJK in Figure 2. Here HIJ is the cylinder and G,K are points at infinity on the x-axis. Consider also the curvilinear coordinate system (α,β) shown in Figure 2. This is supposed to be derived from the Cartesian system by a conformal transformation of the type

$$\alpha + i\beta = F(x + iy). \qquad (8)$$

The transformation is chosen so that the cylinder HIJ corresponds to $\alpha = 0$ and the parts JK, GH of the x-axis correspond to $\beta = 0$, $\beta = \pi$ respectively. The region D above GHIJK therefore corresponds to the interior of the semi-infinite rectangle shown in Figure 3.

Under the conformal transformation (8), equation (3) becomes

$$\nabla_1^2\psi = \zeta/H^2 \tag{9}$$

and equation (4) becomes

$$\frac{\partial\zeta}{\partial t} = H^2(R^{-1}\nabla_1^2\zeta + \frac{\partial\psi}{\partial\alpha}\frac{\partial\zeta}{\partial\beta} - \frac{\partial\psi}{\partial\beta}\frac{\partial\zeta}{\partial\alpha}) \ . \tag{10}$$

Here

$$\nabla_1^2 = \partial^2/\partial\alpha^2 + \partial^2/\partial\beta^2$$

and

$$H^2 = (\partial\alpha/\partial x)^2 + (\partial\alpha/\partial y)^2 = (\partial\beta/\partial x)^2 + (\partial\beta/\partial y)^2.$$

The use of transformations of this kind is well established in the literature. Payne [7] and Kawaguti and Jain [8] have used the particular case

$$F(x + iy) = \log(x + iy) \tag{11}$$

for which

$$H^2 = e^{-2\alpha} \tag{12}$$

in calculations of the time-dependent flow past a circular cylinder. Here $\alpha = 0$ corresponds to the cylinder $x^2 + y^2 = 1$. Apelt [9] and Keller and Takami [10] have used the same transformation in calculations of the corresponding steady flow ($\partial\zeta/\partial t = 0$ in equation (10)). The case of steady flow past a finite flat plate occupying the region $|x| \leq 1$ of the x-axis has been considered by Janssen [11] and by Dennis and Dunwoody [12] using the particular case

$$F(x + iy) = \cosh^{-1}(x + iy)$$

for which

$$H^2 = 2/(\cosh 2\alpha - \cos 2\beta).$$

In this case $\alpha = 0$ corresponds to the plate. Other transformations of the same type can be employed to correspond to cylinders of various other shapes, e.g. the generalized Joukowski aerofoil.

Finally, it remains to state boundary conditions appropriate to the transformed (α,β)-plane of Figure 3. Obviously the first condition of (7) will depend upon the particular transformation used. For the other conditions of (7) we use the relation between the derivatives

$$\left.\begin{aligned} \frac{\partial\psi}{\partial\alpha} &= \frac{\partial x}{\partial\alpha}\frac{\partial\psi}{\partial x} + \frac{\partial y}{\partial\alpha}\frac{\partial\psi}{\partial y} \\ \frac{\partial\psi}{\partial\beta} &= \frac{\partial x}{\partial\beta}\frac{\partial\psi}{\partial x} + \frac{\partial y}{\partial\beta}\frac{\partial\psi}{\partial y} \quad . \end{aligned}\right\} \tag{13}$$

Provided that the derivatives of x and y with regard to α and β remain finite at $\alpha = 0$, we can therefore take

$$t \geq 0: \ \psi = \partial\psi/\partial\alpha = 0 \text{ when } \alpha = 0. \tag{14}$$

For the conditions at infinity it may be observed that for both of the particular cases cited above we can deduce, using (13), that

$$\left.\begin{aligned} t \geq 0: \ e^{-\alpha}\partial\psi/\partial\alpha &\to k\sin\beta \\ e^{-\alpha}\partial\psi/\partial\beta &\to k\cos\beta, \text{ as } \alpha \to \infty. \end{aligned}\right\} \tag{15}$$

Here k is a numerical constant such that $k = 1$ for a circular cylinder and $k = \frac{1}{2}$ for a flat plate. For other types of cylinders, e.g. the Joukowski aerofoil already mentioned, the same conditions (15) hold and we shall take (14) and (15) to be general conditions governing the problem. As a consequence of the uniform stream condition at infinity, it follows that for all time

$$\zeta \to 0 \text{ as } \alpha \to \infty. \tag{16}$$

Lastly, since symmetrical conditions have been assumed, both ψ and ζ must vanish on GH, JK (Figure 2) for all time, viz.

$$\psi = \zeta = 0, \text{ when } \beta = 0,\pi. \tag{17}$$

Next, consider the formulation of these problems in terms of finite differences. For the problem of flow past a cylinder we must

limit the semi-infinite domain in Figure 3 by an artificial boundary. This is designated by the line XY and it corresponds to the curve C_1 mentioned in the introduction. For both problems we now have a finite rectangle OXYZ as the domain D of the numerical solution. A typical set of points on a rectangular grid is shown in Figure 4. The spacing in the two directions is not assumed necessarily to be the same and we write $r^* = h^2/h_1^2$. Only the equations (9) and (10) need be considered. The case H = 1 corresponds to equations (3) and (4).

If we use customary central-difference approximations to second derivatives (see e.g. Fox [13]), the usual approximation to equation (9) is

$$\psi_1 + \psi_3 + r^*(\psi_2 + \psi_4) - (2 + 2r^*)\psi_o - h^2\zeta_o/H_o^2 = 0. \qquad (18)$$

The approximation to equation (10) depends upon whether an explicit or implicit scheme in time is adopted. This is not of great importance in the present report and we illustrate with the simple first-order explicit scheme. If this scheme is adopted we can write, at the typical point 0,

$$\zeta_o(t + \Delta t) = \zeta_o(t) + H_o^2 R^{-1} L_o \Delta t/h^2 \qquad (19)$$

where L_o is an expression in differences. For simplicity write

$$2\lambda = -R\partial\psi/\partial\beta, \quad 2\mu = R\partial\psi/\partial\alpha. \qquad (20)$$

Then if, for example, the ζ-derivatives are expressed in central differences, we have as an approximation

$$\begin{aligned} L_o = {} & (1 + h\lambda_o)\zeta_1 + (1 - h\lambda_o)\zeta_3 \\ & + r^*\{(1 + h_1\mu_o)\zeta_2 + (1 - h_1\mu_o)\zeta_4\} - (2+2r^*)\zeta_o. \end{aligned} \qquad (21)$$

These equations are sufficient to carry out the process described in the introduction. Stage (i) can be carried out at all internal grid

points using (19). At boundaries where ζ is known, e.g. OX, YZ and XY (using (16) as an approximation) in Figure 3, there exists no problem. It clearly cannot be carried out at the boundary OZ in Figure 3, or at any boundary in Figure 1. Stage (ii) is carried out by solving, using boundary-value methods, the matrix problem defined by the equations (18) with known conditions for ψ on the boundaries. In the problem of closed cell flow, $\psi = 0$ on all boundaries. In the cylinder problem, $\psi = 0$ on all except XY. The condition on XY will be considered later. One possibility is to use the first of the conditions (15) as a slope boundary condition on XY.

Finally, in stage (iii), ζ is calculated at any boundary where it is not known. For example, at the boundary OZ in Figure 3, the central difference approximation to the condition $\partial\psi/\partial\alpha = 0$ gives, approximately,

$$\psi_1 = \psi_3 .$$

Also

$$\psi_o = \psi_2 = \psi_4 = 0$$

and hence (18) gives

$$\zeta_o = 2H_o^2\psi_1/h^2 , \qquad (22)$$

which determines ζ at any point on this boundary in terms of the computed internal values of ψ. In this problem this is the only boundary at which ζ must be so determined. It is hardly necessary to give the corresponding equations for finding ζ on the other boundaries of Figure 1. Thus from the given initial state, and with time steps Δt chosen according to some suitable stability criterion, the solution of either problem can be continued indefinitely.

METHOD OF SOLUTION

Consider now some modifications to the method of solution of

equation (9). The cylinder problem is particularly suitable. Since $\psi = 0$ when $\beta = 0$ and $\beta = \pi$ for all t, we may assume the Fourier expansion

$$\psi(\alpha,\beta,t) = \sum_{n=1}^{\infty} f_n(\alpha,t) \sin n\beta \tag{23}$$

satisfying these conditions. Term-by-term differentiation with regard to β is justified (see e.g. Jeffreys and Jeffreys [14]). If we substitute this series into (9) and multiply by the general term $\sin n\beta$ and integrate from $\beta = 0$ to $\beta = \pi$, we obtain the equations

$$f_n'' - n^2 f_n = r_n(\alpha,t), \tag{24}$$

where

$$r_n(\alpha,t) = \frac{2}{\pi}\int_0^{\pi} (\zeta/H^2)\sin n\beta \, d\beta. \tag{25}$$

The equations hold for $n = 1,2,3,\ldots$ and the primes denote differentiation with regard to α, i.e. $f_n' = \partial f_n/\partial\alpha$. Effectively we can treat these equations as ordinary differential equations. Although the time is present in the solutions it enters only through its presence in the quantities $r_n(\alpha,t)$. The integration of equations (24) is carried out at a fixed time and hence we can think of the solutions as dependent only on α at this fixed time.

The boundary conditions for equations (24) follow from (14) and (15). For all values of n

$$f_n = f_n' = 0 \text{ when } \alpha = 0, \tag{26}$$

and, as $\alpha \to \infty$,

$$e^{-\alpha} f_n \to k\delta_n, \quad e^{-\alpha} f_n' \to k\delta_n \tag{27}$$

where $\delta_1 = 1, \ \delta_n = 0 \ (n \neq 1)$.

These conditions can now be used along with the equations (24) to deduce a necessary condition on $r_n(\alpha,t)$ which holds for all values of

the time. Let

$$p_n(\alpha,t) = f_n' + nf_n. \tag{28}$$

Then

$$\frac{\partial}{\partial\alpha}\{e^{-n\alpha}p_n(\alpha,t)\} = e^{-n\alpha}r_n(\alpha,t)$$

and hence

$$e^{-n\alpha}p_n(\alpha,t) = \int_0^\alpha e^{-nz}r_n(z,t)dz, \tag{29}$$

since $p_n = 0$ when $\alpha = 0$. Now let $\alpha \to \infty$ in (29). From (27) we find that

$$\int_0^\infty e^{-nz}r_n(z,t)dz = 2k\delta_n. \tag{30}$$

Consider how the result (30) may be used in the step-by-step time integration previously described. Let stage (i) be completed using, say, the scheme (19). Then ζ is known everywhere except on $\alpha = 0$ and $r_n(\alpha,t)$ can be found from (25) for corresponding values of α. If these values are substituted into (30), using a formula of numerical quadrature, we can determine $r_n(0,t)$ for any required value of n. In practice the upper limit in the integral in (30) is replaced by the finite value α_m corresponding to the boundary XY in Figure 3.

Having found $r_n(0,t)$, the vorticity on the boundary $\alpha = 0$ can be found from the series which results from the inversion of (25), viz.

$$\zeta(\alpha,\beta,t) = H^2 \sum_{n=1}^{\infty} r_n(\alpha,t) \sin n\beta. \tag{31}$$

We thus determine ζ at $\alpha = 0$ without explicitly integrating the equations (24), i.e. stage (iii) is completed before stage (ii). The essential point now is that since $r_n(\alpha,t)$ is known for all stations α, including $\alpha = 0$, the equations (24) can be integrated by initial-value techniques with (26) as initial conditions. From the computed f_n we can calculate $\psi(\alpha,\beta,t)$ and stage (i) is entered again.

The treatment of the closed cell problem is similar. In order to preserve comparability with the analysis just given we shall take the specific dimensions $OZ = \pi$, $OX = \ell$ in Figure 1. With the change in variables of x for α, y for β and with $H = 1$, equations (23), (24) and (25) hold good. The second and last of the boundary conditions (6) now give rise to the conditions

$$f_n = f_n' = 0 \text{ when } x = 0, \ell \tag{32}$$

for the functions $f_n(x,t)$. Equation (29) holds if we put $\alpha = x$. From (32), $p_n = 0$ when $x = \ell$ and hence

$$\int_0^{\ell} e^{-nz} r_n(z,t)dz = 0. \tag{33}$$

Let us introduce the function

$$q_n(x,t) = f_n' - nf_n. \tag{34}$$

We easily deduce the equation

$$e^{nx} q_n(x,t) = \int_0^{x} e^{nz} r_n(z,t)dz, \tag{35}$$

using the equations (24) and the condition that $q_n = 0$ when $x = 0$. Finally, since $q_n = 0$ when $x = \ell$, then

$$\int_0^{\ell} e^{nz} r_n(z,t)dz = 0. \tag{36}$$

The two equations (33) and (36) serve the same purpose in this problem as the single equation (30) in the previous problem. For given n, each may be expressed as a formula of numerical quadrature. Then, given $r_n(x,t)$ for every station x except $x = 0$ and $x = \ell$, two simultaneous equations are obtained to determine $r_n(0,t)$ and $r_n(\ell,t)$. With this additional information it is possible to solve the equations (24) using step-by-step methods.

In practice several new points occur in this problem. One is that

$\zeta(x,0,t)$ and $\zeta(x,\pi,t)$ are nonzero and, further, they will be unknown at the stage when $r_n(x,t)$ is evaluated. If conventional methods of numerical quadrature are used to evaluate $r_n(x,t)$, no additional problem occurs. The integrand of the integral in equation (25) is zero at the end points and the values of ζ at these points do not affect the integration. However, it is found that specialized formulae have to be used for the integration and this does create difficulties in the problem of flow in the closed cell. We shall return to this later. Another point in this problem is that it is not possible to use the equation (31) to determine ζ on the boundaries $y = 0$ and $y = \pi$ even when $r_n(x,t)$ is known. The series on the right does not converge to the function on the left at these points unless ζ is zero there, i.e. we get the Gibbs phenomenon. It would be surprising if it were possible because we have not yet utilized the slope boundary conditions for ψ on $y = 0,\pi$. This point also will briefly be considered later.

NUMERICAL ANALYSIS

Two problems must be considered, the evaluation of the integral in (25) just mentioned, and the solution of the equations (24) by step-by-step methods. Each presents some difficulty if treated by conventional methods and we shall consider them in turn.

The problem with the integral on the right side of (25) is that unless a very fine grid is used in the β(or y) direction the result of conventional numerical quadrature will be inaccurate when n is large and the periodic function has many zeros in the range. Filon [15] pointed this out and proposed special formulae for such cases. The principle is based on polynomial approximation to the nonperiodic part of the integrand only, rather than to the whole integrand. Filon gives

details when the approximating polynomial is a parabola over three successive equally-spaced values of the integrand. For the integral on the right side of (25) the result, for integration over the points 2, 0, 4 shown in Figure 4, is

$$\int_{\beta_4}^{\beta_2} \zeta \sin n\beta \, d\beta = \frac{1}{n}(\zeta_4 \cos n\beta_4 - \zeta_2 \cos n\beta_2)$$
$$+ \frac{1}{2h_1 n^2}\{(3\zeta_4 - 4\zeta_o + \zeta_2)\sin n\beta_4 + (\zeta_4 - 4\zeta_o + 3\zeta_2)\sin n\beta_2\}$$
$$- \frac{1}{h_1^2 n^3}(\zeta_4 - 2\zeta_o + \zeta_2)(\cos n\beta_4 - \cos n\beta_2). \qquad (37)$$

The integral over the range $\beta = 0$ to $\beta = \pi$, assuming an even number of intervals, is obtained by summing this result.*

Filon integration permits evaluation of $r_n(\alpha,t)$ with good accuracy when n is large but it does create the difficulty that the function needs to be known at the end points. This presents a problem only in the case of the closed cell flow. We shall consider this point later.

Next consider the solution of the equations (24) using step-by-step methods. It is convenient to drop the subscripts and also to consider the solutions as functions of a single variable, say x, i.e. we consider them at fixed time. Thus we consider the single equation

$$f'' - n^2 f = r(x) \qquad (38)$$

and, to start, consider the solution defined in the finite range $x = 0$

---

* For further details of this result, including the error term, see the National Bureau of Standards Handbook of Mathematical Functions (Seventh Printing, May 1968) p. 890 together with the footnote, p. 890. The form we give in equation (37) is equivalent to Filon's actual form, but expressed differently.

to $x = \ell$ with the conditions (corresponding to (32))

$$f(0) = f'(0) = 0 \tag{39a}$$

$$f(\ell) = f'(\ell) = 0. \tag{39b}$$

We assume $r(x)$ to be given at all grid points on the interval $x = 0$ to $x = \ell$, including the end points. At this stage also we shall abandon the notation of the points in Figure 4 and suppose that a typical grid point in the x-direction is denoted by $x_m = mh$ ($m = 0,1,2,\ldots$) and that f_m denotes $f(x_m)$.

In theory, only the initial conditions (39a) are necessary to integrate (38) as a step-by-step problem. However, most step-by-step procedures applied to this problem are unsatisfactory, particularly if n is large. For example, the direct second-order approximation using central differences gives the approximation

$$f_{m+2} = h^2 r_{m+1} + (2 + n^2h^2)f_{m+1} - f_m. \tag{40}$$

With some starting procedure which gives f_1, equation (40) can be used to construct an approximate solution starting from $m = 0$, but an elementary error analysis (see Forsythe and Wasow [16]) indicates that the error propagation is unsatisfactory. The error at some fixed value of x is unbounded as $h \to 0$ for all values of n. Also, for fixed h the error at fixed x increases rapidly with n. In the present application it is obvious that h will remain fixed regardless of n so that this latter property makes the use of a formula such as (40) unsuitable. To some extent the error growth is associated with the presence of the increasing exponential term $\exp(nx)$ in the complementary function of (38). This term plays little part in the required solution (in the cylinder problem it obviously, from the conditions (27), plays no part if $n > 1$) so the error growth is unacceptable. For the same reason any

attempt to express the equation (38) as two simultaneous first-order equations with known initial conditions leads to a basically unsatisfactory system.

As an example, consider the two first-order equations obtained by using the functions given by equations (28) and (34). The function $p(x)$ (using the notation of the present section) satisfies the equation

$$p' - np = r(x) \tag{41}$$

and $q(x)$ satisfies

$$q' + nq = r(x). \tag{42}$$

The initial conditions are $p(0) = q(0) = 0$. If we express the first derivatives by simple forward differences, an approximation to (41) (the Euler method) is

$$p_{m+1} = (1 + nh)p_m + hr_m \tag{43}$$

and to (42)

$$q_{m+1} = (1 - nh)q_m + hr_m . \tag{44}$$

The error growth associated with (43) and (44) can be discussed following the analysis given by Forsythe and Wasow. That associated with (43) will be unacceptable, but that associated with (44) may be acceptable. The reason is that the unwanted increasing exponential part of the complementary function of (38) has been isolated in (41) and the decreasing part in (42).

In the present application, however, we not only have initial conditions for $p(x)$ and $q(x)$ but also the conditions $p(\ell) = q(\ell) = 0$, i.e. more conditions than are theoretically needed. With the aid of these a satisfactory procedure can be constructed. Equation (42) is integrated in the increasing x-direction with initial condition $q(0) = 0$. Equation (41) is integrated backwards with $p(\ell) = 0$. An

equivalent way of looking at the latter integration is to put $x = \ell - z$ in (41) whence it becomes

$$dp/dz + np = -r(\ell - z), \tag{45}$$

with initial condition

$$p = 0 \text{ when } z = 0. \tag{46}$$

Equation (45) is now of the same character for increasing argument as equation (42) and the error growth is at least tolerable.

From the functions $p(x)$ and $q(x)$ computed in this way, $f(x)$ and $f'(x)$ are obtained from the equations

$$\left.\begin{aligned} f &= (p - q)/2n \\ f' &= (p + q)/2 \ . \end{aligned}\right\} \tag{47}$$

Also, a highly sensitive check on the numerical procedure can now be made. It is that f and f' computed from (47) must now come out to be zero (within an acceptable numerical tolerance) at both $x = 0$ and $x = \ell$. Moreover, this cannot possibly happen unless the conditions (33) and (36) have been correctly satisfied. The check therefore tests this in addition to the accuracy of the step-by-step process and is a severe one.

It is now clear from the above that we may restrict further consideration to the question of constructing an approximation to equation (42) with the initial condition $q(0) = 0$. A detailed error analysis of the approximation (44) indicates that, although the approximation is satisfactory in a manner not shared by the approximation (43), it cannot be expected to be effective unless nh is small compared with 1. We certainly cannot expect to obtain an accurate solution unless this condition is satisfied. Since h is fixed and n may be large this will

not in general be satisfied. A method must be constructed which does not, on the whole, lose accuracy as n increases. Such a method is suggested by the principle of Filon quadrature.

We denote as before the value $x = mh$ by x_m and the corresponding value $q(x_m)$ by q_m. Equation (42) may be written

$$\frac{d}{dx}\{e^{nx}q(x)\} = e^{nx}r(x)$$

whence

$$q(x) = e^{-n(x-x_m)}q_m + e^{-nx}\int_{x_m}^{x} e^{n\xi}r(\xi)d\xi. \qquad (48)$$

If $x = x_m + sh$, this formula is a multi-step formula for the step-by-step integration of equation (42). The integral extends over s steps and we suppose in the usual way that r(x) is approximated by a polynomial P(x) passing through some, or all, of the corresponding s+1 points and perhaps also through points outside the range. The question of error propagation due to this approximation is now considered. Propagation of round-off error is not explicitly considered but a very similar analysis can be given to cover this type of error.

Let the error of the polynomial approximation at the point ξ be

$$E(\xi) = r(\xi) - P(\xi). \qquad (49)$$

Let $q^*(x)$ satisfy (48) when r(x) is approximated by P(x) and let

$$\varepsilon(x) = q(x) - q^*(x) \qquad (50)$$

denote the error. Then

$$\varepsilon(x) = e^{-n(x-x_m)}\varepsilon_m + T(x), \qquad (51)$$

where T(x) is the truncation error defined by

$$T(x) = e^{-nx}\int_{x_m}^{x} e^{n\xi}E(\xi)d\xi. \qquad (52)$$

Various estimates of T(x) can be made, for example, a crude estimate is obtained by assuming only that r(x) is continuous on the interval (x_m,x). By definition E(x) is continuous on the same interval and thus

$$T(x) = E(\xi_1)\ \{1 - e^{-n(x-x_m)}\}/n, \tag{53}$$

where $x_m < \xi_1 < x$. Thus T(x) cannot exceed the maximum error of the interpolating polynomial for any value of n.

Only the cases s = 1, s = 2 will be considered in detail as these are of the most value in practical integrations. The case s = 1 gives a one-step integration. Equation (51) becomes

$$\varepsilon_{m+1} = e^{-nh}\ \varepsilon_m + T_{m+1}\ , \tag{54}$$

where the last term denotes $T(x_{m+1})$. The solution is

$$\varepsilon_m = \gamma^m \varepsilon_o + S_m\ , \tag{55}$$

where

$$\gamma = e^{-nh}$$

$$S_m = \sum_{j=1}^{m} \gamma^{m-j} T_j\ .$$

If $\hat{T}$ is the magnitude of the numerically greatest of T_j then

$$|S_m| \le \hat{T}(1 - \gamma^m)/(1 - \gamma). \tag{56}$$

From equation (55) we have the following simple properties of error propagation. For given h, $\gamma < 1$ and the error after m steps is bounded as $m \to \infty$. Moreover, as $h \to 0$ the error at a fixed value $x = mh$ remains bounded since $\gamma^m \to e^{-nx}$. For convergence, suppose x_o is the initial point x = 0 and that the initial condition (actually q = 0 in the present application) has been calculated exactly. Then $\varepsilon_o = 0$ and convergence is established if $S_m \to 0$ as $h \to 0$ for fixed $x = mh$. Clearly $S_m \to 0$ if $\hat{T} \to 0$. From (53), for all m,

$$T_{m+1} \sim hE(\xi_1)$$

and $E(\xi_1)$ certainly remains bounded. Thus $\hat{T} \to 0$. Actually, as is well known, if $P(x)$ passes through the $j + 1$ points

$$x_i, x_{i+1}, \cdots, x_{i+j}$$

and $r(x)$ possesses continuous derivatives up to order $j+1$ on an interval which contains these points and the argument ξ, then

$$E(\xi) = (\xi - x_i)(\xi - x_{i+1})\ldots(\xi - x_{i+j})r^{(j+1)}(\eta)/(j+1)! \quad (57)$$

where η lies on the given interval. In this case $E(\xi_1) = 0(h^{j+1})$ as $h \to 0$.

The formula for q^* for the one-step case is

$$q^*_{m+1} = e^{-nh}q^*_m + e^{-nx_{m+1}} \int_{x_m}^{x_{m+1}} e^{n\xi}P(\xi)d\xi. \quad (58)$$

The simplest form for $P(\xi)$ is to take it constant, i.e.

$$P(\xi) = r(x_m) = r_m.$$

This corresponds directly to the Euler formula in the approach using standard difference methods. The approximation obtained from (58) is

$$q^*_{m+1} = e^{-nh}q^*_m + r_m(1 - e^{-nh})/n \ . \quad (59)$$

If we assume the expression (57) for the error, with $i = m$ and $j = 0$ in this case, substitution in (52) yields

$$T_{m+1} = e^{-nx_{m+1}} \int_{x_m}^{x_{m+1}} (\xi - x_m)r'(\eta)\ e^{n\xi}d\xi. \quad (60)$$

If we apply the mean value theorem then

$$T_{m+1} = e^{-nx_{m+1}}\ r'(\eta_1) \int_{x_m}^{x_{m+1}} (\xi - x_m)e^{n\xi}d\xi, \quad (61)$$

where $x_m < \eta_1 < x_{m+1}$. We can deal with (61) in two ways, firstly by evaluation of the integral, which yields

$$T_{m+1} = \frac{r'(\eta_1)}{n}\{h - (1 - e^{-nh})/n\} \ . \quad (62)$$

Alternatively, we can again employ the mean value theorem to give

$$T_{m+1} = \frac{1}{2} e^{n(\xi_1 - x_{m+1})} h^2 r'(\eta_1) , \qquad (63)$$

where $x_m < \xi_1 < x_{m+1}$. The two forms clearly become equivalent if, for fixed n, $h \to 0$. However, in general they display different properties. Equation (62) exhibits a tendency for the truncation error to decrease with n. Equation (63) indicates that, regardless of n, the truncation cannot exceed $h^2 r'(\eta_1)/2$, which is what it would be if the Euler method were applied to integrate the basic differential equation (42) with n = 0.

A similar situation exists if $P(\xi)$ is taken as the straight line joining x_m to x_{m+1}. The truncation error is then

$$T_{m+1} = \frac{1}{2!} e^{-nx_{m+1}} \int_{x_m}^{x_{m+1}} (\xi - x_m)(\xi - x_{m+1}) r''(\eta) e^{n\xi} d\xi$$

and it is easily shown that T_{m+1} cannot exceed in magnitude the term $-h^3 r''(\eta_1)/12$, where $x_m < \eta_1 < x_{m+1}$. This term gives the truncation error when trapezoidal integration is applied to the special case n = 0 of equation (42). We can clearly write down a formula of similar type for the truncation error when $P(\xi)$ is a polynomial of any degree. However, the general investigation of this error is then more difficult. In particular, the term $E(\xi)$ changes sign over the range of integration and the process of getting simple estimates of the kind just given is more involved. Although the point has not been investigated fully it does seem to be possible, following methods used by Steffensen [17] in the theory of numerical quadrature, to establish the following result. For any given polynomial approximation $P(\xi)$ to $r(\xi)$ in (48), the magnitude of the truncation error (52) does not exceed the magnitude

of the corresponding truncation of numerical quadrature when n = 0.

We turn finally to the actual formulae utilized in the numerical work of this study. Two formulae have been used, the first a one-step formula to effect the first step of the integration from the initial point x_o to the point x_1, but using parabolic approximation to r(x) over the points x_o, x_1, x_2. The second formula used was the two-step formula obtained by putting $x = x_m + 2h$ in (48) and using parabolic approximation for r(x) over the successive points x_m, x_{m+1}, x_{m+2}. The appropriate formulae for q* are as follows. For the first of these two

$$q^*_1 = \gamma q^*_o + \frac{1}{n}(r_1 - \gamma r_o) - \frac{1}{2hn^2}\{r_2 - r_o - \gamma(4r_1 - 3r_o - r_2)\} + \frac{1}{h^2 n^3}(r_o - 2r_1 + r_2)(1 - \gamma), \quad (64)$$

where γ is as previously defined. For the second

$$q^*_{m+2} = \gamma^2 q^*_m + \frac{1}{n}(r_{m+2} - \gamma^2 r_m) - \frac{1}{2hn^2}\{(3r_{m+2} - 4r_{m+1} + r_m) - \gamma^2(4r_{m+1} - 3r_m - r_{m+2})\} + \frac{1}{h^2 n^3}(r_m - 2r_{m+1} + r_{m+2})(1 - \gamma^2). \quad (65)$$

The resemblance between (65) and the Filon quadrature formula (37) is obvious.

The question of error propagation for two-step formulae such as (65) may be considered in a similar manner to that in the one-step case. The error equation is

$$\varepsilon_{m+2} = \gamma^2 \varepsilon_m + T_{m+2}, \quad (66)$$

where T_{m+2} is given by putting $x = x_{m+2}$ in (52). Actually the only new point is that (66) has two independent solutions, one for even values of m generating from the initial value ε_o and the other for odd values of m generating from ε_1. The general error propagation pro-

perties of these two solutions are essentially similar to those discussed in the one-step case and need not be considered further. In practice, ε_1 will be determined by the starting approximation to q. This can be obtained using any one-step formula, such as (64). Generalization of these results to the multi-step case is obvious and we shall give no further discussion of this.

The truncation error T_1 in (64) is obtained by putting m = 0, $x = x_1$ in the formula (52). Also $E(\xi)$ is given by (57) with i = 0, j = 2. The polynomial part of $E(\xi)$ does not change sign over the range of integration so it is easy to deduce that $T_1 = e^{n(\xi_1-h)}h^4r'''(\eta_1)/24$, where $0 < \xi_1 < h$ and $0 < \eta_1 < 2h$. For the two-step formula (65), $E(\xi)$ is given by putting i = m, j = 2 in (57). In this case the polynomial part of $E(\xi)$ does change sign over the range of integration. This case has not been investigated fully but, as previously noted, it is believed that the truncation can be shown to be not greater in magnitude than that obtained by putting n = 0 in (52). This would give the truncation not greater in magnitude than that of the Simpson formula applied to the function r(x) over the same interval.

Finally some results are given of a specific numerical illustration of the whole computational procedure of solving equation (38) subject to the boundary conditions (39a) and (39b). Some computations were carried out to test the method. In this test r(x) was taken to be

$$r(x) = 100 + ae^{-x/2} + be^{-3x/2},$$

with a(n) and b(n) chosen to satisfy the necessary conditions (33) and (36). The range of integration was taken as $\ell = 1$. Equation (42) was integrated in the positive x-direction and equation (41) in the negative

x-direction as already described. Both integrations were carried out using formulae of type (64) and (65), equation (64) being used for the first step and (65) being used to continue the integration.

Computations were carried out for integer values of n from n = 1 to n = 20. For each case two approximate solutions were obtained using h = 0.1, 0.05 respectively and the results compared with the known exact solution. This comparison was found to be extremely satisfactory. In Table 1 some comparisons are given for one value only, the value f(0.5), but on the whole the result is representative of those obtained over the complete range. The values are given in floating decimal form.

n	Exact	h = 0.1	h = 0.05
1	1.87926E-01	1.87641E-01	1.87925E-01
5	1.19699E-01	1.19699E-01	1.19699E-01
10	5.65582E-02	5.65622E-02	5.65584E-02
15	3.04646E-02	3.04671E-02	3.04647E-02
20	1.86811E-02	1.86827E-02	1.86811E-02

TABLE 1. Values of f(0.5)

The main evidence of this table is that for a given grid size the approximations maintain their accuracy as n increases. This is in agreement with the theory and confirms the essential object of the method. A few other features of the numerical solutions obtained may be summarized as follows. For the grid size h = 0.05, the solutions computed using the step-by-step process agree with those computed from the exact solution to 5 or 6 decimal places at every grid point for every value of n from n = 1 to n = 20. In this case also, the check that f(0) and f(1) should both come out zero was satisfied to at least

a tolerance of 10^{-5}, and more often 10^{-6} or 10^{-7}. For the grid size $h = 0.1$ this tolerance was rather greater, varying from 10^{-4} to 10^{-6}. In both cases this check improves as n increases.

Finally, some discussion of the solution of (38) must be given in the case which corresponds to flow past a cylinder. Although, in practice, the range of integration is still a finite number ℓ (corresponding to the imposed boundary XY in Figure 3), in theory this range is infinite in this problem. The new point is that the boundary conditions (39b) are not now available. Although in theory only the conditions (39a) are required to solve the step-by-step problem, some replacement for (39b) must obviously be made if the methods described above are to be used. No new problem exists for the integration of (42) since the initial condition $q(0) = 0$ is still known. We do, however, require to know $p(\ell)$ in order to initiate the backward integration of (41).

To consider the problem properly we should first examine the nature of the time-dependent solution of (10) for large α in order to ensure that the determination of $r_n(\alpha,t)$ from (25) is such that, as $\alpha \to \infty$, the integral in the condition (30) converges at its upper limit. This would establish that the problem is properly posed and also provide information on the assumption to be made for $p(\ell)$. The investigation is difficult for the time-dependent problem but it can be carried out for steady motion, and the results give some idea of what to assume for time-dependent flow. We shall therefore consider the solution of the steady-state problem before considering this point.

SOLUTION OF THE STEADY-STATE EQUATIONS

If we put $\partial\zeta/\partial t = 0$ in equation (10) it becomes

$$\nabla_1^2 \zeta = R\left(\frac{\partial\psi}{\partial\beta}\frac{\partial\zeta}{\partial\alpha} - \frac{\partial\psi}{\partial\alpha}\frac{\partial\zeta}{\partial\beta}\right). \tag{67}$$

In order to determine a steady flow configuration it is necessary to obtain a solution $\zeta(\alpha,\beta)$ of this equation together with a solution $\psi(\alpha,\beta)$ of equation (9). The steady-state boundary conditions are given by (6) for flow in a rectangular cell and by equations (14), (15), (16) and (17) in the case of flow past a cylinder. All time-dependent quantities which have previously been defined are now independent of time and we can use the same notation, e.g. $r_n(\alpha)$ now defines the left side of (25) when $\zeta(\alpha,\beta)$ is implied in the right side.

The central-difference approximation to (67) at the typical point 0 of Figure 4 is $L_o = 0$, viz.

$$\begin{aligned}(1 + h\lambda_0)\zeta_1 + (1 - h\lambda_0)\zeta_3 \\ + r^*\{(1 + h_1\mu_0)\zeta_2 + (1 - h_1\mu_0)\zeta_4\} - (2+2r^*)\zeta_0 = 0.\end{aligned} \tag{68}$$

The only essentially new point in the steady-state problem is that the set of equations (68) now defines a problem of boundary-value type for determining ζ within the region OXYZ of Figure 1 or Figure 3 rather than the step-by-step problem given by (19). In order to solve these equations it is necessary to specify a boundary condition for ζ at all points of the boundary OXYZ. Except at points where a specific condition is given, e.g. on OX, XY and YZ in Figure 3 but on none of the boundaries in Figure 1, boundary values of ζ must be calculated as part of an iterative scheme of solving the problem. The scheme is very similar to that employed in the time-dependent case and consists of obtaining a sequence of iterates $\psi^{(m)}(\alpha,\beta)$, $\zeta^{(m)}(\alpha,\beta)$, $(m = 1,2,3,\ldots)$

which converge to numerical solutions of (9) and (67) and satisfy all the boundary conditions.

Following the procedure for the time-dependent case, the present method of solution employs the equations (68) to approximate equation (67), while the Poisson equation (9) is solved by the step-by-step method already described. Consider the problem of flow past a cylinder. The iterative procedure is as follows. A given iterate $\zeta(\alpha,\beta)$ (omitting the superscript for convenience) is obtained by solving the matrix problem (68) for grid points internal to OXYZ. Approximations to the boundary values $\zeta(0,\beta)$ on OZ required for this calculation have already been determined, and the necessary values of λ and μ have been calculated from the most recent iterate for ψ. From the new values of ζ it is now possible to calculate $r_n(\alpha)$ from (25) for all grid lines parallel to OZ and for any value of n. This permits the calculation of new estimates of $r_n(0)$ from (30) or, more precisely (since the integration range is finite in practice), from

$$\int_0^{\alpha_m} e^{-nz} r_n(z)dz = 2k\delta_n . \tag{69}$$

The calculation can be expressed approximately in the form

$$hw_o r_n(0) = 2k\delta_n - h \sum_{j=1}^{m} w_j e^{-njh} r_n(jh) . \tag{70}$$

Here the factors w_j are the weighting coefficients of the quadrature formula which is used to approximate the integral and $\alpha_m = mh$, corresponding to the boundary XY.

The calculated values of $r_n(0)$ are used, through (31), to determine boundary values of ζ on OZ for the next iterate. Also the step-by-step integration of the equations (24) can be carried out to determine,

through the series (23), the iterate for $\psi(\alpha,\beta)$. A complete cycle of processes has now been carried out and this can be repeated until convergence. As in the time-dependent case, it may be noted that the calculation of boundary values for ζ is carried out independently from the determination of the iterate for ψ. Thus the method again differs from the usual finite-difference procedure in which the equations (18) are used to determine ψ and the new boundary condition for ζ calculated from (22), in which case the internal solution for ψ must be known in order to calculate ζ on OZ. To some extent the independence of the calculation of the new boundary condition for ζ and the iterate for ψ adds flexibility to the iterative method of solution, but we shall not elaborate on this point.

It has been noted in the literature (see, for example, Thom and Apelt [18]) that the process of solving the equations (18) and (68) iteratively with the boundary condition for ζ calculated by (22) can be divergent. Suppose an iterate $\zeta^{(m)}(\alpha,\beta)$, with boundary condition $\zeta^{(m)}(0,\beta)$ on OZ, gives rise to a new iterate for $\psi(\alpha,\beta)$ from which a new boundary condition, say $\zeta^*(0,\beta)$, is calculated using (22). Divergence of the repeated iterations can be caused if $\zeta^*(0,\beta)$ is taken as the boundary condition $\zeta^{(m+1)}(0,\beta)$ for the next iterate. It is therefore customary to calculate the new boundary condition from the relation

$$\zeta^{(m+1)}(0,\beta) = \kappa\zeta^*(0,\beta) + (1-\kappa)\zeta^{(m)}(0,\beta), \tag{71}$$

where $0 < \kappa \leq 1$, and it is usually possible to ensure convergence of the iterations by taking κ small enough. The process, frequently termed smoothing, can be used equally well in the present method of

solution. Various elaborations of this process and other devices for accelerating convergence have been described in the literature. Many are considered in references already cited. Greenspan [19] has also suggested some techniques in an investigation of the steady flow in a rectangular cavity. Many of these devices are applicable to the present method.

In order to investigate the convergence of the integral in (30) it is necessary to obtain the form of the solution of (67) for large α. From the details it is possible to determine an assumption for $p(\ell)$ which may be applied on the boundary XY. It is also possible to obtain a very much better approximation to a boundary condition for ζ on XY than the very crude assumption that (16) holds at the finite distance $\alpha = \alpha_m$. The solution for large α is found by linearizing equation (67) with the boundary conditions (15) satisfied by ψ as $\alpha \to \infty$. This is the Oseen method of linearization (see Lamb [20]).

If the boundary conditions (15) for ψ are substituted in (67) it assumes the limiting form

$$\nabla_1^2 \zeta = \mathrm{Rke}^{\alpha}\left(\cos\beta \frac{\partial \zeta}{\partial \alpha} - \sin\beta \frac{\partial \zeta}{\partial \beta}\right), \tag{72}$$

valid for large α. A complete solution of this equation which satisfies the necessary conditions that $\zeta = 0$ when $\beta = 0$ and $\beta = \pi$ can be verified to be

$$\zeta(\alpha,\beta) = e^{\chi\cos\beta} \sum_{m=1}^{\infty} A_m K_m(\chi) \sin m\beta, \tag{73}$$

where

$$\chi(\alpha) = \mathrm{Rke}^{\alpha}/2$$

and K_m is the modified Bessel function of the second kind. The constants $A_m (m = 1,2,3,\ldots)$ are arbitrary. They cannot be determined explicitly

without further information, e.g. a knowledge of the complete solution of (67) in a domain which overlaps the domain of validity of (73).

Since χ is large when α is large and the leading term of the asymptotic expansion of $K_m(\chi)$ for large χ is

$$K_m(\chi) \sim (\pi/2\chi)^{\frac{1}{2}} e^{-\chi},$$

then for large α equation (73) can be replaced by

$$\zeta(\alpha,\beta) \sim G(\beta)\chi^{-\frac{1}{2}} \exp\{\chi(\cos\beta - 1)\}, \qquad (74)$$

where $G(\beta)$ is a function of β alone given by

$$G(\beta) = (\pi/2)^{\frac{1}{2}} \sum_{m=1}^{\infty} A_m \sin m\beta. \qquad (75)$$

Equation (74) gives the character of the steady-state vorticity distribution for large α. It is exponentially small except in a region lying between $\beta = 0$ and the curve

$$\chi(1 - \cos\beta) = \beta_o^2 ,$$

where β_o is a number whose choice depends upon how small ζ is required to be on the curve in order to be counted as negligible. Since this equation clearly makes β small for large χ, we can replace it approximately by the equation

$$\beta = \beta_o(2/\chi)^{\frac{1}{2}}. \qquad (76)$$

Consider now the determination of $r_n(\alpha)$ from (25) when α is large. The region within which the vorticity is significant is limited by the curve (76) for which β decreases proportionately to $\chi^{-\frac{1}{2}}$ as $\alpha \to \infty$. Suppose χ is taken large enough so that the expressions $\sin n\beta$, $\cos\beta - 1$ and $\sin m\beta$ which occur, respectively, in equations (25), (74) and (75) can be replaced by their leading terms for small β. It should be borne in mind that we are only in practice concerned with a finite number of terms of the various series involved so that the question of making

this approximation for large values of m and n, for which χ would have to be very large, is not really relevant. Let us also make the change of variable

$$\beta = (2/\chi)^{\frac{1}{2}}\theta,$$

so that the region of significant vorticity lies between $\theta = 0$ and $\theta = \beta_o$. Then as $\alpha \to \infty$ equation (25) can be replaced by

$$r_n(\alpha) \sim \frac{4nS}{\chi^2\pi^{\frac{1}{2}}} \int_o^\infty H^{-2}\theta^{-2}e^{-\theta^2}d\theta. \qquad (77)$$

In this expression

$$S = \sum_{m=1}^{\infty} mA_m$$

and is assumed to converge. In practice it is approximated by a finite number of terms.

The quantity H in (77) is the asymptotic form as $\alpha \to \infty$ of the corresponding quantity in (25). For the case of a circular or elliptic cylinder

$$H^{-2} \sim k_1 e^{2\alpha}, \text{ as } \alpha \to \infty,$$

where k_1 is a constant. This behavior is standard for the type of transformation considered here. It holds, for example, in the case of the generalized Joukowski aerofoil. If we assume this result to be generally true, substitution in (77) gives finally

$$r_n(\alpha) \to nc, \text{ as } \alpha \to \infty \qquad (78)$$

where

$$c = 4k_1 S/R^2 k^2$$

and is definite constant for a given cylinder shape at a given Reynolds number. The result (78) was obtained in the case of a flat plate using somewhat similar methods by Dennis and Dunwoody and it was shown that the constant c can be expressed in terms of the total drag force exerted by the fluid on the plate. A similar result can be obtained in the more general case considered here.

The limit (78) indicates that, for fixed n, the integral in the condition (30) converges at its upper limit. It also indicates ultimate divergence of the series (31) as $\alpha \to \infty$, but the practical situation for large but finite α is that (31) converges very slowly. In fact, the limit nc for $r_n(\alpha)$ is approached more slowly as n increases, corresponding to the fact that the replacement of sin $n\beta$ by $n\beta$ in (25) is valid only for small $n\beta$, i.e. α must be larger as n increases, since the maximum β is given by (76). The slow convergence does not seriously affect the numerical process since (31) is used only at $\alpha = 0$, where the convergence is quite satisfactory in numerical examples.

In order to consider the boundary condition to be applied on XY in Figure 3 let $\alpha = x$, to keep the notation of the previous section, and suppose that $x = \ell$ corresponds to XY. It may be recalled that there is no new problem in solving (42) since the condition $q(0) = 0$ still applies. In view of (78) the numerical procedure of solving (42) will, if continued for large enough x, determine a solution in which $q(x) \to c$ as $x \to \infty$. To deal with equation (41), we multiply by e^{-nx} and integrate from $x = \ell$ to $x = \infty$. Thus

$$2k\delta_n - e^{-n\ell}p(\ell) = \int_\ell^\infty e^{-nx}r(x)dx ,$$

where δ_n has the meaning defined in (27). If we integrate the right side by parts and rearrange, then

$$p(\ell) = 2k\delta_n e^{n\ell} - \frac{r(\ell)}{n} - \frac{1}{n}\int_\ell^\infty e^{n(\ell-x)}r'(x)dx. \qquad (79)$$

The last term on the right side of (79) can be written as $-r'(\xi)/n^2$, where $\xi > \ell$. By equation (78), this term may be neglected if ℓ is large enough, giving the approximation

$$p(\ell) = 2k\delta_n e^{n\ell} - r(\ell)/n. \qquad (80)$$

To some extent the approximation can be tested by an estimation of the error term, taking $\xi = \ell$ and calculating $r'(\ell)$ using numerical differentiation. If necessary the process can be continued by further integration of the last term on the right side of (79), e.g.

$$p(\ell) = 2k\delta_n e^{n\ell} - r(\ell)/n - r'(\ell)/n^2,$$

the error term now being $- r''(\xi_1)/n^3$, where $\xi_1 > \ell$. In the actual calculations which have been carried out, the approximation (80) has been found to be satisfactory for the following reason.

The reason is related to the question of approximating the infinite integral in (30) and we shall deal with this latter point first. Because of the nature of the limit (78), some error may be incurred by replacing the upper limit by the finite number ℓ, particularly for small values of n. The approximation can be improved by assuming that ℓ has been taken large enough so that (78) is a good approximation for $\alpha \geq \ell$, at least for the smaller values of n. If we make this approximation in the integral, we can replace the condition (30) by the condition

$$\int_0^\ell e^{-nz} r(z)dz = 2k\delta_n - ce^{-n\ell}. \qquad (81)$$

The constant c is determined from the relation

$$c = r(\ell)/n.$$

Consider next the approximation to $p(\ell)$. One of the important requirements of the backward integration of (41) is that p(x) shall come out zero at $x = 0$. If we multiply (41) by e^{-nx} as before and integrate from $x = 0$ to $x = \ell$, we have

$$p(\ell)e^{-n\ell} - p(0) = \int_0^\ell e^{-nz} r(z)dz .$$

The integral on the right side may now be replaced by the right side

of (81). It is found that the necessary condition for $p(0) = 0$ is

$$p(\ell) = 2k\delta_n e^{n\ell} - c.$$

This is exactly consistent with the approximation (80) and it is extremely satisfactory that the improved approximation to the infinite integral in (30) together with the use of this approximation to $p(\ell)$ shall lead to the satisfaction of the necessary condition $p(0) = 0$. In the numerical work it has been found that the condition $p(0) = 0$ is satisfied to very good precision using the above scheme.

The nature of the expression (74) which approximates $\zeta(\alpha,\beta)$ for large α indicates a very slow decay of vorticity in the wake of the cylinder, i.e. in the region for which β is less than the value given by the curve (76). Within this region the approximation $\zeta = 0$ on the boundary $\alpha = \alpha_m$, i.e. the boundary which must necessarily be imposed in a numerical calculation, will be a poor approximation. If it is assumed that α_m is taken large enough for (74) to be a reasonable approximation for $\alpha \geq \alpha_m$, we can utilize this expression to provide a boundary condition on $\alpha = \alpha_m$. This is done by assuming (74) to be valid on the successive grid lines $\alpha = \alpha_m$ and $\alpha = \alpha_m + h$. The unknown function $G(\beta)$ is then eliminated from the two resulting equations, which gives the approximation

$$\zeta(\alpha_m + h,\beta) = \zeta(\alpha_m,\beta) \exp\{(\chi_{m+1} - \chi_m)(\cos\beta - 1) - h/2\}. \qquad (82)$$

Here χ_m denotes the value of χ at $\alpha = \alpha_m$ and χ_{m+1} that at $\alpha = \alpha_m + h$.

Equation (82) is used as a boundary condition in conjunction with the set of equations (68). Once a value for α_m has been assigned, the exponential on the right side can be calculated for all values of β and the equation is similar to a gradient boundary condition. It may be used, following the usual manner for a gradient-type condition, to

eliminate values of ζ external to OXYZ from the equations (68). The values of ζ at grid points on $\alpha = \alpha_m$ are determined as part of the solution. The treatment given here is similar in principle to that given in a recent paper by Dennis, Hudson and Smith [21] in a problem of steady heat convection.

Keller and Takami, in their investigation of the steady flow past a circular cylinder, use a procedure in which the solution of Imai [22], valid for large α, is utilized to calculate approximate boundary values for both ζ and ψ on $\alpha = \alpha_m$. In order to obtain explicit values, the coefficient C_D corresponding to the drag exerted by the fluid on the cylinder must be known. This is not known, but an approximation to it can be obtained corresponding to any approximation to ζ and ψ which has been obtained within OXYZ. Keller and Takami's procedure therefore uses Imai's solution to calculate, from an approximation to C_D, approximations to ζ and ψ on $\alpha = \alpha_m$. The difference equations (18) and (68) are then solved within OXYZ. This leads to a better estimate of C_D and the process is then repeated iteratively until convergence. It may be noted that a similar explicit procedure for calculating $\zeta(\alpha_m, \beta)$ according to (74) could be adopted in the present method. For large α, equation (74) is equivalent to

$$\zeta \sim A\chi^{-1}\theta e^{-\theta^2}, \tag{83}$$

where $A = \pi^{\frac{1}{2}}S$ and S, θ are as previously defined. The constant S can be expressed in terms of C_D by considering the flux of momentum across a large enough contour surrounding the cylinder. However, the use of (74) in the form (82) is more satisfactory since it does not require explicit calculation of C_D.

Although Imai's solution represents a higher order approximation to the Navier-Stokes equations than that given by the Oseen theory, the question of whether its use as a boundary condition in the present case will lead to a more accurate solution is worth considering. For large α the vorticity is significant only within the boundary defined by (76). Within this boundary it may be assumed to be given approximately by equation (83). Let us examine the relative magnitudes of the terms in equation (72) within this region, i.e. for fixed θ and large α. From (83) we obtain the results (noting that θ is a function of both α and β)

$$\left.\begin{aligned} \partial\zeta/\partial\alpha &\sim -A\theta(\theta^2 + \tfrac{1}{2})\chi^{-1}e^{-\theta^2} \\ \partial\zeta/\partial\beta &\sim A(2\chi)^{-\frac{1}{2}}(1 - 2\theta^2)e^{-\theta^2}. \end{aligned}\right\} \qquad (84)$$

Within the given region the terms $\cos\beta$ and $\sin\beta$ may be replaced by the values 1 and β respectively. Thus for fixed θ and as $\alpha \to \infty$, the two terms in the bracket on the right side of (72) each tend to zero like χ^{-1} and the whole right side tends to a function of θ alone. By further differentiation of the expressions (84) it is found that $\partial^2\zeta/\partial\beta^2$ tends to a function of θ alone as $\alpha \to \infty$, but that $\partial^2\zeta/\partial\alpha^2$ tends to zero like χ^{-1}.

The situation for large α is therefore that three terms in equation (72) balance and that the fourth, the term $\partial^2\zeta/\partial\alpha^2$, tends to zero. Equation (72) therefore becomes effectively a first-order equation in the α-direction. Since it is the limit equation of (67) for large α, the same tendency is exhibited by the latter equation. Its numerical solution is therefore relatively insensitive to the downstream boundary condition and is almost a continuation problem in the α-direction. The lack of dependence of the numerical solution on the downstream boundary

condition has been observed in numerical examples solved by present methods.

A similar situation occurs in the numerical determination of the stream function ψ as $\alpha \to \infty$. In numerical studies it is quite customary to introduce a perturbation stream function which measures the difference between ψ and the stream function of the potential flow past the cylinder. For large α the potential flow must satisfy the conditions (15), and it is sufficient for present purposes to define a perturbation Ψ by the equation

$$\psi = \Psi + ke^{\alpha}\sin\beta. \tag{85}$$

Obviously, Ψ satisfies the same equation (9) as ψ. For large α we assume, as before, that $H^{-2} \sim k_1 e^{2\alpha}$ and also that ζ is given by (83). In this case Ψ satisfies the equation

$$\nabla_1^2 \Psi = (4Ak_1/R^2k^2)\chi\theta e^{-\theta^2} \tag{86}$$

as $\alpha \to \infty$. Within the region of significant vorticity β is small for fixed θ, and $\partial^2/\partial\beta^2 = (\chi/2)\partial^2/\partial\theta^2$. A solution of (86), valid within this region, can now be obtained by balancing the term $\partial^2\Psi/\partial\beta^2$ with the term on the right side, so that Ψ satisfies

$$\partial^2\Psi/\partial\theta^2 = (8Ak_1/R^2k^2)\theta e^{-\theta^2}. \tag{87}$$

The solution must satisfy $\Psi = 0$ when $\theta = 0$. Outside the vorticity wake, where $\zeta = 0$, it must match the harmonic function $B(1 - \beta/\pi)$ which satisfies the other required condition that $\Psi = 0$ when $\beta = \pi$. The necessary solution of (87) is

$$\Psi = (-4Ak_1/R^2k^2)\int_0^{\theta} e^{-z^2} dz. \tag{88}$$

The constant A can be expressed in terms of B, but there is no need to give further details.

The variable θ is a function of both α and β. Differentiation of (88) indicates that, in the region of significant vorticity, $\partial^2\psi/\partial\alpha^2$ tends to a function of θ alone and $\partial^2\psi/\partial\beta^2$ tends to infinity like χ, as $\alpha \to \infty$. Hence $\partial^2\psi/\partial\alpha^2$ is asymptotically small with regard to $\partial^2\psi/\partial\beta^2$, verifying that (87) is a valid approximation to (86) for large α. The resulting solution (88) is equivalent, in the present coordinate system, to the leading term of Imai's solution. However, the important point is that (87) requires no boundary condition in the α-direction. The approximation to Ψ for large α is generated by integration along grid lines parallel to $\alpha = 0$ from a knowledge of ζ on these lines. This is exactly consistent with the approximation (80) to $p(\ell)$. The term involving $e^{n\ell}$ which is present when $n = 1$ corresponds to the effect of the potential term on the right side of (85), while the term involving $r(\ell)$ depends only on an integration in the β-direction.

Although the present discussion is appropriate only to the steady-state problem, the approximations to the outer boundary conditions can be extended intuitively to the time-dependent case. In the early stages of the motion, although $\partial\zeta/\partial t$ in equation (10) is large near the cylinder, very little diffusion of vorticity into the outer region has taken place and the external flow is still approximately potential. The approximations (80) and (82) take some account of this diffusion and are probably better than the assumption of potential flow on $\alpha = \alpha_m$. Moreover as the wake builds up it does so, although at first its strength is weak, in the same basic form indicated by equation (74) with which the approximations (80) and (82) are consistent. This feature, together with the fact that the procedure described ensures that $p(0,t)=0$,

tends to justify its use for all values of the time.

The present section has been centered on the problem of flow past cylinders. In the problem of flow in a rectangular cell there is no difficulty in specification of the boundary conditions, but certain other difficulties arise in the present method of solution. One is the point already mentioned that if Filon quadrature is used to evaluate r_n from (25), values of ζ must be known at the ends of the range of integration. This presents no real problem for the steady-state integrations. Here a sequence of iterates $\zeta^{(m)}(\alpha,\beta)$ $(m = 1,2,3,\ldots)$ is determined and the most recently available values of ζ may be used to define the integrand on the right side of (25). The second difficulty, also previously mentioned, is that even when r_n has been determined for sufficient n and for all grid lines in $0 \leq x \leq \ell$, the series (31) cannot be used to calculate ζ on $y = 0,\pi$ although it can be used on $x = 0,\ell$ if $0 < y < \pi$. The simplest way out of this difficulty is to use the series (23) to calculate ψ at all grid points neighboring the boundary OXYZ in Figure 1 and then calculate ζ on this boundary using the appropriate finite-difference relations of type (22). All the boundary conditions are satisfied and the explicit integration of the Poisson equation is still achieved.

This latter method can also be used to calculate the boundary vorticity in the time-dependent case, but a slight difficulty still exists in this problem. Suppose the solution has been completed everywhere through time t. Equation (19) then gives $\zeta_o(t + \Delta t)$ at every internal grid point but not on $y = 0,\pi$. It is needed on these boundaries if $r_n(x,t + \Delta t)$ is to be obtained by Filon quadrature. Whereas in the steady case boundary values from the previous iterate can be used, since

we are interested only in the final limit solution, in this case it is not consistent to use values of $\zeta(x,0,t)$, $\zeta(x,\pi,t)$ in the calculation if the actual time development of the solution is required. However, Δt is usually small to ensure a stable integration, so the use of $\zeta(x,0,t)$ and $\zeta(x,\pi,t)$ will give a good approximation to $r_n(x,t + \Delta t)$. The equations (24) can then be solved and a good approximation to $\psi(x,y,t + \Delta t)$ obtained at all internal grid points from (23). This approximation may then be introduced into the difference equations (18) and improved, if necessary, using one of the usual iterative methods. From the solution which results, ζ at time $t + \Delta t$ may be calculated on the boundaries from relations of type (22). The iterative solution of the Poisson equation (3) is not entirely eliminated in this case, but the time spent on it is reduced.

In subsequent sections some calculated results for flow past cylinders are given. Some have been obtained by solving the equations of steady motion and some by time-dependent integrations, although in the latter case only the final steady results to which the solutions converge are given. In the time-dependent problem an impulsive start to the motion was employed. There are a number of points of interest to be considered in this problem and a full discussion will be given in a later report. One point only is considered here, the question of how the motion is started in practice.

INITIAL MOTION FOR FLOW PAST CYLINDERS

The initial conditions in this problem require further discussion. The first condition of (7) for $t < 0$ is not really relevant to the problem. At the instant $t = 0$ at which the cylinder is brought to rest relative to the fluid, an infinitesimally thin boundary layer (see

Schlichting [23]) is formed at the surface of the cylinder. At this instant the conditions $\psi = \partial\psi/\partial\alpha = 0$ apply at the cylinder surface and the solution for ψ within the boundary layer may be obtained by solving the time-dependent boundary-layer equations. Outside the boundary layer the stream function may be taken as that for the potential flow past the cylinder. For small values of t the thickness of the boundary layer grows proportionately to $(t/R)^{\frac{1}{2}}$. The initial variation of vorticity on the surface of the cylinder is proportional to $(t/R)^{-\frac{1}{2}}$. Thus at $t = 0$ an infinitesimally thin ring of vorticity of infinite magnitude is generated at the surface of the cylinder.

To start an integration it is necessary to postulate initial values for ζ on the boundary OZ. This is usually done by assuming an initial distribution $\psi(\alpha,\beta,0)$, e.g. that of potential flow past the cylinder, and calculating ζ on OZ from (22). For finite h this necessarily gives a finite starting distribution $\zeta(0,\beta,0)$ for the vorticity which cannot be in agreement with the correct solution. The point has been noted by Payne and more recently by Ingham [24]. Actually, it can be shown that not only is the initial calculation of ζ from (22) unsatisfactory, but also that it is incorrect to assume any initial distribution of ψ in equation (10) other than that consistent with the solution inside the boundary layer.

The boundary-layer solution indicates that the term $\partial^2\zeta/\partial\beta^2$ in (10) is initially small compared with $\partial^2\zeta/\partial\alpha^2$. Also the convection terms on the right side of (10) are initially small since $\psi = \partial\psi/\partial\alpha = 0$ at the cylinder surface. The initial solution of (10) comes from the balance of terms

$$\frac{\partial \zeta}{\partial t} = R^{-1} H_o^2 \frac{\partial^2 \zeta}{\partial \alpha^2} , \tag{89}$$

where H_o is the value of H at the cylinder surface. This is a function of β alone and hence if we put $t = RT/H_o^2$ then (89) becomes

$$\frac{\partial \zeta}{\partial T} = \frac{\partial^2 \zeta}{\partial \alpha^2} . \tag{90}$$

A solution of (90) can now be found in the form

$$\zeta = T^{-\frac{1}{2}} F(z,\beta)$$

where

$$\alpha = 2zT^{\frac{1}{2}}$$

and $F(z,\beta)$ satisfies the equation

$$\frac{\partial^2 F}{\partial z^2} + 2z \frac{\partial F}{\partial z} + 2F = 0.$$

A solution of this equation which satisfies the condition that $\zeta \to 0$ as $z \to \infty$ is $F = e^{-z^2}$. However, ζ must vanish on $\beta = 0, \pi$. The function

$$F(z,\beta) = e^{-z^2} \sin n\beta$$

satisfies the equation for all values of n and hence a complete solution for ζ can be expressed in the form

$$\zeta = T^{-\frac{1}{2}} \sum_{n=1}^{\infty} B_n e^{-z^2} \sin n\beta, \tag{91}$$

where the B_n are constants to be determined.

The constants B_n are found from (30), which is an exact condition for the problem. Firstly, $r_n(\alpha,t)$ is found from (25). The result depends upon the specific function of β which defines H_o in a given case, but, having found $r_n(\alpha,t)$, substitution in (30) gives a set of linear algebraic equations to determine B_n. For example, for a circular cylinder, $H_o = 1$ and

$$r_n(\alpha,t) = B_n T^{-\frac{1}{2}} e^{-\alpha^2/4T}.$$

It follows from (30) that

$$B_n = 0, \quad (n = 2,3,4,\ldots).$$

The condition for n = 1 determines B_1, with k = 1 in this case. For small times, the boundary layer is confined to a small thickness in α. The exponential in (30) can be replaced by unity and we find that $B_1 = 2/\pi^{\frac{1}{2}}$, and the initial solution for the vorticity is

$$\zeta = 2(R/\pi t)^{\frac{1}{2}} \exp(-R\alpha^2/4t)\sin\beta. \tag{92}$$

Obviously, it is impossible to specify ζ numerically at t = 0. Moreover, the vorticity distribution given by (92) cannot be represented adequately for small times by any finite-difference scheme. Ingham's work on the circular cylinder indicates that the most satisfactory procedure is to start the integration using the boundary-layer solution and continue it using numerical methods. The stream function $\psi(\alpha,\beta,t)$ in the boundary layer for small t can be obtained from (9). Initially $\partial^2\psi/\partial\beta^2$ is small compared with $\partial^2\psi/\partial\alpha^2$ and, for small α, H can be approximated by H_o. The initial stream function satisfies

$$\frac{\partial^2\psi}{\partial\alpha^2} = \zeta/H_o^2$$

and if the expression (91) for ζ is substituted, the equation can be integrated twice with regard to α subject to the conditions that $\psi = \partial\psi/\partial\alpha = 0$ at $\alpha = 0$. For a circular cylinder, using (92), the expression

$$\psi(\alpha,\beta,t) = 4(t/R)^{\frac{1}{2}} \{\eta\,\mathrm{erf}\eta + \frac{1}{\sqrt{\pi}}(e^{-\eta^2} - 1)\} \sin\beta, \tag{93}$$

where $\eta = (R/t)^{\frac{1}{2}}\alpha/2$, results. Here erf$\eta$ is the error function defined by

$$\mathrm{erf}\eta = \frac{2}{\sqrt{\pi}} \int_o^\eta e^{-z^2}\,dz.$$

In the present coordinate system, the above expressions are equivalent to the boundary-layer solution (Goldstein and Rosenhead [25]). They are valid for any Reynolds number for small enough time. Outside

the boundary layer the flow is approximately potential. For very small times the boundary layer is very thin and although the integration can be started using the above analysis, there are still some substantial difficulties in continuing it numerically.

Essentially the reason is that h must be small in the thin boundary layer, and consequently Δt must be small. In fact, if the explicit forward-difference scheme in time used in equation (19) is applied to the equation (89) governing the initial vorticity distribution, the condition for stability is

$$\Delta t \leq Rh^2/2H_m^2 , \tag{94}$$

where H_m is the maximum value of H_o. The point has been well illustrated from a practical point of view by Ingham's recent calculations. It is obvious that very small grid sizes and time steps must be taken to get an accurate initial flow. Since the accuracy of the subsequent flow, except in the final steady state, must depend upon the initial flow, the problem of impulsively started flows requires further investigation.

CALCULATION OF THE FLOW PAST A CIRCULAR CYLINDER

All lengths are assumed to have been made nondimensional with respect to the radius a of the cylinder and all velocities with respect to the constant stream velocity U. The details of the transformation (8) are as given by (11) and (12). The dimensionless stream function and negative vorticity which appear in equations (9) and (10) are related to the dimensional stream function and vorticity, ψ' and ζ', by the equations $\psi' = Ua\psi$, $\zeta' = -U\zeta/a$. The time t in (10) is U/a times the actual time and the Reynolds number R is Ua/ν. Actually it is more usual to use a Reynolds number $Re = 2Ua/\nu$ based on the diameter of the cylinder and we shall adhere to this. Thus $R = Re/2$ is substituted in (10).

Two separate investigations of this problem have been carried out.

Firstly, the time-dependent method was used to calculate the flow from the impulsive start for Re = 7, 10, 20 and 40. The calculations were continued until a steady state was reached and details of the steady-state results which were obtained have already been given by Dennis and Chang [26]. No details of the time-dependent results were given, since the problem has been thoroughly investigated by Kawaguti and Jain and the present results are in good agreement. Kawaguti and Jain take grid sizes $h = h_1$ and use the stability condition

$$\Delta t \leq Rh^2/4H_m^2 \tag{95}$$

which assumes that equation (10) can be treated as a simple heat conduction equation with the nonlinear terms neglected and with H taking its greatest value H_m. The condition (94) suggests that, initially anyway, Δt can be twice as large. In the present calculations it was found that larger time steps could be taken than implied by (95) and the integrations remained stable for all times. The time steps used in the calculations are shown in Table 2 of Ref. [26], together with other parameters which were used.

Time-dependent solutions were also attempted for Re = 100 and subsequently for Re = 70. In order that Δt should not be too small, the solution for Re = 100 was first obtained using coarse grid sizes $h = h_1 = \pi/40$, and with $\Delta t = 0.05$. A steady-state solution was reached satisfactorily but it was distorted in the wake in a manner thought to be physically unrealistic, i.e. the thickness and length of the wake increased unreasonably. The same undoubtedly would have been true of Kawaguti and Jain's integration at this Reynolds number had it been allowed to continue to a steady state, for they used the coarser grid $h = h_1 = \pi/30$. Similar features appear to be present in the recent results of Son and Hanratty [27] at Re = 200 and 500.

The attempt at Re = 100 was followed by an attempt at Re = 70 using $h = h_1 = \pi/60$, $\Delta t = 0.03$. This was found to approach a realistic steady solution, and the case Re = 100 was then attempted again with the same spatial and time steps as for Re = 70. This was also approaching a realistic steady solution, but very slowly. This slow ultimate approach to the steady solution is a feature of time-dependent flow. Kawaguti and Jain, also Son and Hanratty, have experienced it and have discontinued some integrations before a steady solution was reached. Certain steady properties, e.g. drag coefficients, were then estimated by extrapolation. The present solutions for Re = 70 and 100 were also terminated before the final limit was reached. The late time solutions were then used to start the iterative solution of the steady equations of motion; the solutions for steady flow were found in this way.

The only steady flow results beyond Re = 40 are the recent calculations of Takami and Keller [28], who have given results up to Re = 60.* There is still considerable interest in an accurate description of the nature of the steady flow as the Reynolds number increases. A direct investigation of the steady problem by present methods has been carried out for the range of Reynolds numbers, and for the values of the parameters, shown in Table 2. Here, n_o is the number of terms used to approximate the series in (23). The general iterative procedure of solution which has already been described was used, with smoothing of boundary values of ζ according to (71). The values of κ used are given in Table 2. Convergence was satisfactory with these values, although they are not necessarily the largest values consistent with convergence.

---

* Recently, some results have been reported by Hamielec and Raal [45]; they are briefly described at the end of the Appendix.

Re	$h = h_1$	α_m/π	n_o	κ
5	$\pi/40$	1	20	0.05
7	$\pi/40$	1	20	0.05
10	$\pi/40$	1	20	0.05
20	$\pi/40$	1	30	0.05
40	$\pi/40$	1	30	0.05
70	$\pi/60$	7/6	40	0.03
100	$\pi/60$	7/6	40	0.015

TABLE 2. Parameters of steady calculations

The two values of α_m correspond respectively to dimensionless radial distances of approximately 23.1 and 39.1 from the center of the cylinder. The larger value was taken at the two highest Reynolds numbers in view of the increasing wake length at the rear of the cylinder. In all cases it was found (by observing the effect of varying α_m) that this boundary was far enough from $\alpha = 0$ for the approximations (80) and (82) to be satisfactory. As predicted by theory, the solution for $\alpha < \alpha_m$ is extremely insensitive to the conditions assumed on $\alpha = \alpha_m$.

A simple Gauss-Seidel iterative procedure was used to solve the difference equations (68), using a definite number of sweeps (say 40 or 50) of the complete field to define a given iterate $\zeta^{(m)}(\alpha,\beta)$ rather than obtaining a fully converged solution of (68) to some imposed accuracy. In this way the only convergence test which needs to be considered is on the overall procedure of determining the successive iterates $\zeta^{(m)}(\alpha,\beta)$, $\psi^{(m)}(\alpha,\beta)$. The following was found to be satisfactory. By its definition through equations (70) and (25) each $r_n(0)$,

i.e. the value of $r_n(\alpha)$ on OZ, is determined from values of $\zeta(\alpha,\beta)$ throughout the whole domain. The procedure was assumed to have converged when two successive iterates of $r_n(0)$ agreed to some assigned tolerance for all values of n up to n_o. This ensures convergence of the boundary condition for ζ on OZ.

In order to obtain numerical solutions of the greatest possible accuracy, the final solutions which were obtained using the finite-difference equations (68) were subsequently improved using a difference correction method similar to that proposed by Fox [29]. If L_o denotes the left side of (68), the equation $L_o = 0$ is the result of neglecting third and fourth differences and above in the central-difference formulae for the first and second derivatives of ζ with regard to α and β in (67). If we include third and fourth differences at the typical point 0 as a correction K_o, equation (68) becomes

$$L_o + K_o = 0. \tag{96}$$

It is easily verified that the formula for K_o is

$$\begin{aligned} 12K_o = {} & 4(1 + h\lambda_o)\zeta_1 + 4(1 - h\lambda_o)\zeta_3 - (1 + 2h\lambda_o)\zeta_9 \\ & -(1 - 2h\lambda_o)\zeta_{11} + r^*\{4(1 + h_1\mu_o)\zeta_2 + 4(1 - h_1\mu_o)\zeta_4 \\ & -(1 + 2h_1\mu_o)\zeta_{10} - (1 - 2h_1\mu_o)\zeta_{12}\} - 6(1 + r^*)\zeta_o \ . \end{aligned} \tag{97}$$

If the grid sizes have been chosen properly the correction K_o, evaluated using the converged solution which satisfies $L_o = 0$, should be small throughout the field. An improved solution can then be calculated by setting up a new iteration which includes the correction. If in the old iteration without correction a given iterate $\zeta^{(m)}(\alpha,\beta)$ is obtained by solving the difference equations $L_o^{(m)} = 0$, a suitable

scheme for the new iteration is to solve the equations

$$L_o^{(m)} + K_o^{(m-1)} = 0, \tag{98}$$

i.e. the vector K_o is calculated from the previous iterate $\zeta^{(m-1)}(\alpha,\beta)$ and held fixed during the determination of the new iterate $\zeta^{(m)}(\alpha,\beta)$. This is the basis of Fox's correction method. If K_o is everywhere small, the procedure (98) will converge to (96), in which L_o and K_o are mutually consistent. If K_o is not everywhere small the indication is that the grid sizes are too large.

There is no difficulty in calculating the correction K_o at any point of the computational field. On grid lines adjacent to $\beta = 0$ and $\beta = \pi$ the formula (97) involves values of ζ which lie outside the field of computation OXYZ, but these can be expressed in terms of internal values of ζ from the relations

$$\zeta(\alpha, -\beta) = -\zeta(\alpha,\beta), \quad \zeta(\alpha, \pi + \beta) = -\zeta(\alpha, \pi - \beta)$$

which hold because the flow is symmetrical about the x-axis. External values of ζ are also involved when K_o is calculated on XY and on the adjacent grid line $\alpha = \alpha_m - h$, but in this case the solution for $\alpha > \alpha_m$ can be extrapolated using (74). Finally, if the typical point 0 is on the grid line $\alpha = h$ the value ζ_{11} is external to the field. In this case since from (67) $\nabla_1^2\zeta = 0$ when $\alpha = 0$ then, approximately,

$$\zeta_{11} = 2(1 + r^*)\zeta_3 - \zeta_0 - r^*(\zeta_6 + \zeta_7),$$

so that ζ_{11} can be calculated from internal and boundary values of ζ.

Application of this method to the results obtained using (68) yielded only a small correction for all Reynolds numbers, which suggests that the final results are of good accuracy. In previous calculations of the steady flow, only Apelt at Reynolds number 40 has taken into account higher difference corrections to (68) by a somewhat different method

from that used here. The grid size ($h = h_1 = \pi/20$) of Apelt's calculation is rather coarse.

The final results for the streamlines of the steady flow in the seven cases considered are shown in Figures 5 - 11. Numerical values indicate values of the dimensionless stream function ψ. Separation of the flow to form a recirculating region behind the cylinder has just started at Reynolds number 7 and the length of this wake grows approximately in proportion to the Reynolds number thereafter. The growth of the length of this region with Reynolds number is one of the major points of interest. Previous numerical solutions indicate a linear growth with Reynolds number. There are one or two exceptions to this, e.g. the solutions of Allen and Southwell [30] and Dennis and Shimshoni [31], but in both of these there are probably deficiencies in the numerical procedures when the Reynolds number becomes large. Takami and Keller's recent work gives approximately linear growth up to Re = 60. Son and Hanratty do not obtain the steady wake length.

The present results are compared with previous numerical results and with the experimental estimates of Taneda [32] and Acrivos, Leal, Snowden and Pan [33] in Figure 12. The quantity L plotted is the dimensionless distance from the rearmost point of the cylinder to the end of the separated vortex pair; this is also given numerically in Table 3. There is seen to be excellent agreement between the linear trend of the present results and the corresponding tendency of Takami and Keller's calculations. The results of Kawaguti and Jain start to depart from a linear relationship after Re = 20. It seems possible that this is due to the coarseness of their grid. A similar effect was observed in our calculations for the time-dependent flow at Re = 100

using $h = h_1 = \pi/40$. By the time L had reached its steady-state limit it was almost 22, i.e. 11 diameters of the cylinder. Moreover, as previously noted, the vortex region was distorted and had tended to become fat, very much after the manner of Son and Hanratty's results for Re = 200 and 500. The results of Allen and Southwell and also those of Dennis and Shimshoni have been omitted from Figure 12 in view of their doubtful reliability.

The point at which the fluid separates from the surface of the cylinder is determined from the condition that ζ must vanish there. From (31) (or rather the steady analogue of it with the time absent) it follows that the angle of separation $\beta = \beta_s$ is a root of

$$\sum_{n=1}^{\infty} r_n(0) \sin n\beta = 0. \qquad (99)$$

Calculated values of β_s are given in Table 3. They are in extremely good agreement with the calculations of Takami and Keller, who give the respective values $\beta_s = 14.5^\circ$, 29.3°, 43.65°, 53.55°, 56.6°, 59.0° at the Reynolds numbers 7, 10, 20, 40, 50 and 60. Separation first starts to take place at some critical Reynolds number between 5 and 7 for which $\beta_s = 0$. It may be deduced with the aid of (99) that this Reynolds number is that which makes the sum

$$S_1(\mathrm{Re}) = \sum_{n=1}^{\infty} n r_n(0)$$

vanish. From the present results we obtain the approximations $S_1(5) = 0.100$ and $S_1(7) = -0.068$. A linear interpolation suggests the critical Reynolds number as 6.2.

Re	L	β_s	C_f	C_p	C_D	P(0)	P(π)
5	----	----	1.917	2.199	4.116	-1.044	1.872
7	0.19	15.9	1.553	1.868	3.421	-0.870	1.660
10	0.53	29.6	1.246	1.600	2.846	-0.742	1.489
20	1.88	43.7	0.812	1.233	2.045	-0.589	1.269
40	4.69	53.8	0.524	0.998	1.522	-0.509	1.144
70	8.67	61.3	0.360	0.852	1.212	-0.439	1.085
100	13.11	66.2	0.282	0.774	1.056	-0.393	1.060

TABLE 3. Properties of steady solutions

A general formula for the drag on the cylinder has been given in the Appendix. In the present case the dimensionless drag coefficient is defined by $C_D = D/\rho U^2 a$ and it follows that

$$C_D = \frac{4}{Re}\int_o^\pi \zeta_o \sin\beta \, d\beta - \frac{4}{Re}\int_o^\pi (\partial\zeta/\partial\alpha)_o \sin\beta \, d\beta, \qquad (100)$$

where the subscripts here denote values at $\alpha = 0$. The first term on the right gives the friction drag coefficient and the second the pressure drag coefficient, denoted respectively by C_f and C_p. Very simple expressions can be obtained for these quantities by substituting from (31) with $H^2 = e^{-2\alpha}$. We obtain

$$C_f = 2\pi r_1(0)/Re$$

and

$$C_p = 2\pi\{2r_1(0) - r_1'(0)\}/Re \ .$$

where the prime denotes differentiation with regard to α.

Calculated drag coefficients are given in Table 3 and also in Figure 13, where the total drag coefficient is compared with other numerical results and with the experimental measurements of Tritton [34]. Takami and Keller have attempted to correlate their drag values with

the formula

$$C_D^{\frac{1}{2}} \sim C_{D\infty}^{\frac{1}{2}} + \gamma Re^{-\frac{1}{2}} \tag{101}$$

given by Imai [35] on the assumption that the limiting flow for large Reynolds number is of Kirchhoff type. The value $C_{D\infty}$ is the drag coefficient of the limiting Kirchhoff flow and γ is an unknown constant. For a circular cylinder, Brodetsky [36] gives $C_{D\infty} = 0.5$. Takami and Keller estimate γ by evaluating it directly from (101) for Re = 50 and 60 and then extrapolating linearly in 1/Re as $Re \to \infty$. This gives $\gamma = 3.547$.

A similar procedure carried out with the present values at Re = 70 and 100 gives $\gamma = 2.99$. With this value, the formula (101) gives the respective values $C_D = 0.84$, 0.55 at Re = 200, 500. The comparison with the numerical values of 0.924 and 0.60 given at the same respective Reynolds numbers by Son and Hanratty is not particularly good. Moreover, the discrepancy in the value of γ between the present estimation and that of Takami and Keller tends to indicate that no conclusive numerical evidence is yet forthcoming in support of the formula (101). If we assume an asymptotic boundary-layer type expansion for the friction drag in powers of $Re^{-\frac{1}{2}}$ and fit the first two terms to the results for Re = 70, 100 this gives

$$C_f \sim 1.827Re^{-\frac{1}{2}} + 9.949Re^{-1}.$$

This formula not only fits the value at Re = 40 but gives respective values $C_f = 0.18$, 0.10 at Re = 200 and 500. These compare well with the values 0.19 and 0.09 of Son and Hanratty.

The formula for the calculation of the pressure coefficient

$$P(\beta) = 2\{p(\beta) - p_\infty\}, \tag{102}$$

where $p(\beta)$ is the dimensionless pressure on the cylinder surface and p_∞ that at large distances, is given in the Appendix. Curves of the pressure coefficient are given in Figure 14 and its values at the rear ($\beta = 0$) and the front ($\beta = \pi$) of the cylinder are given in Table 3. According to the exact solution for stagnation point flow (see Schlichting [23]) the coefficient at the front of the cylinder should behave for large Reynolds number as

$$P(\pi) \sim 1 + \delta Re^{-1} \tag{103}$$

where δ is a constant. Takami and Keller have estimated $\delta = 5.985$ by calculation from (103) at Re = 50, 60 and extrapolating linearly in 1/Re as $Re \to \infty$. A similar extrapolation from the present results at Re = 70 and 100 yields $\delta = 6.09$, which is in reasonable agreement.

The behavior of the pressure coefficient at the rear of the cylinder is of interest in view of two models which have been proposed for the separated flow at high Reynolds numbers. According to Roshko [37] and to Sychev [38] the behavior for large Reynolds numbers should be

$$P(0) \sim CRe^{-\frac{1}{2}} \tag{104}$$

where C is a constant. On the other hand, the recent measurements of Acrivos et al. suggest that P(0) becomes constant as the Reynolds number increases, in agreement with a previous model proposed by Acrivos, Snowden, Grove and Petersen [39]. The experimental coefficient becomes constant at quite moderate values of the Reynolds number, of the order of 100. Unfortunately, the results of the present calculations do not support either of the above theories and appear to lie somewhere in between. The variation of P(0) is not rapid enough to fit (104). Neither is the coefficient obviously approaching a constant, at least certainly not in the range -0.47 to -0.43 suggested by the experimental results for circular cylinders. This question obviously requires further

elucidation.

The distribution of vorticity throughout the flow field is shown for the two cases Re = 70 and 100 in Figures 15 and 16. For the lower values of Re, the features of the vorticity distributions are essentially those already given by Takami and Keller. The dimensionless negative vorticity on the surface of the cylinder is shown in Figure 17. No reasonable prediction can be made as to its ultimate tendency for large Reynolds number, and in particular as to the ultimate position of the separation point.

Finally, the effect on the solutions of the number n_o was considered in several cases and it was on the basis of the information obtained that the values in Table 2 were used in the final computations. More terms in the series (23) are needed as the Reynolds number increases but the number $n_o = 40$ is still adequate at Re = 100. If we take as an illustration the variation of wake length with n_o at this Reynolds number we find L = 8.12, 12.03 and 12.99 at values n_o = 10, 20, 30. The final value (Table 3) is L = 13.1.

CALCULATED FLOW PAST AN ELLIPTIC CYLINDER

If $F = \cosh^{-1}(x + iy) - \alpha^*$ in (8) a transformation is obtained in which $\alpha = 0$ corresponds to an ellipse whose ratio of minor to major axes is $\tau = \tanh \alpha^*$ and for which $H^2 = 2/\{\cosh 2(\alpha+\alpha^*) - \cos 2\beta\}$. The value of k in (15) is $\frac{1}{2}e^{\alpha^*}$. The present calculations were carried out for $\tau = 1/5$ and for a range of values Re = 1 to 200, where Re is the Reynolds number based on the major axis of the ellipse. A definition of Re in terms of the generalized number R is given on the next page. The time-dependent method was used with the impulsive start from rest, but since one of

the main interests was in the final steady flow it was subsequently found to be necessary to modify the procedure as described below. Only details of the steady-state solutions will be given here.

The dimensionless major axis is of length 2cosh α^* and is parallel to the free stream. If the dimensional major axis is of length 2dcosh α^* and ψ and ζ are related to the dimensional stream function and vorticity, ψ' and ζ', by $\psi' = Ud\psi$, $\zeta' = -(U/d)\zeta$ then $R = Ud/\nu$ in (10). However, it is more convenient to use the number $Re = (2Udcosh\ \alpha^*)/\nu$ based on the major axis of the ellipse and for the purpose of the calculations the substitution $R = Re/(2cosh\ \alpha^*)$ is made in (10). Solutions were obtained for the values of Re in Table 4 on p. 61. A square grid $h = h_1$ was used. Values of h and α_m appropriate to each Reynolds number are given in Table 4. The values of A in this table are defined by equation (107) and other quantities are subsequently defined.

The greatest value of H over all the internal grid points occurs on the line $\alpha = h$, at the points for which $\beta = h$ and $\beta = \pi - h$. If the time step Δt is calculated to satisfy (94), with H_m taken as the greatest internal value of H, and we assume h and α^* to be small then, approximately,

$$\Delta t \leq \tfrac{1}{2}Rh^2\ \{(\alpha^* + h)^2 + h^2\}$$

for stability. For a thin ellipse Δt must be extremely small and a very large number of time steps are necessary to reach the final steady state. If the main interest is in the steady results the process can, however, be accelerated at any stage as follows. The limiting steady solution is independent of the form of H in equation (10). We can therefore take H as, for example, its value $e^{-\alpha}$ for a circular cylinder in (10) (but not, of course, in (9)), and then use time steps

the same as for a circular cylinder. This was found to work and, in fact, all the solutions were ultimately completed using this procedure. Naturally the validity of the time-dependent results is destroyed after this procedure is adopted, since the correct form of equation (10) is not being used. In any case it is not proposed to discuss the time-dependent results in this report. Finally, some of the steady results (at Re = 1, 40, 100 and 200) were checked using the steady method of solution and found to agree satisfactorily. The higher difference correction K_o was not employed for these solutions.

The dimensionless negative vorticity on the surface of the cylinder is shown for the range of Reynolds numbers in Figure 18. As in the case of the circular cylinder, the quantity $\zeta(0,\beta)$ is shown as a function of β and the values have been calculated from (31), which in this case gives

$$\zeta(0,\beta) = \frac{2}{\cosh 2\alpha^* - \cos 2\beta} \sum_{n=1}^{\infty} r_n(0) \sin n\beta. \quad (105)$$

The angle β is not as physically meaningful in this case as it is for the circular cylinder, but it is convenient. A more meaningful coordinate is

$$x^* = x/\cosh \alpha^*$$

which is equal to $\cos\beta$ at points on the ellipse. In particular, if β is small then $\beta \sim [2(1-x^*)]^{\frac{1}{2}}$, i.e. β is proportional to the square root of the distance from the trailing edge of the ellipse measured along the major axis. Likewise if $\pi-\beta$ is small, this angle is proportional to the square root of the distance from the leading edge.

The vorticity passes through a sharp peak in the vicinity of the leading edge. Figure 18 indicates that the peak occurs at approximately

the same value of β independently of Reynolds number. If α^* is small, this can be shown to be so. We put $\beta = \pi - \phi$ in (105), then ϕ is small near the leading edge and, on the cylinder, approximately

$$\zeta \sim \frac{A\phi}{\phi^2 + \alpha^{*2}} \tag{106}$$

where

$$A = \sum_{n=1}^{\infty} (-1)^{n+1} n r_n(0) \tag{107}$$

and depends upon the Reynolds number. The peak occurs where $\partial\zeta/\partial\phi = 0$ and hence from (106) approximately when $\phi = \alpha^*$, with a corresponding maximum value of vorticity $A/2\alpha^*$. In the present case $\alpha^* = 0.2027$ approximately, giving an estimate $\phi = 11.6^o$ for the position of the maximum which agrees remarkably well with the calculated results given in Figure 18.

If D is the total drag on the cylinder, the dimensionless drag coefficient is defined by $C_D = D/(2\rho U^2 d\cosh \alpha^*)$. It is given (see Appendix) by

$$C_D = \frac{2\cosh \alpha^*}{Re} \int_o^{\pi} \zeta_o \sin\beta \, d\beta - \frac{2\sinh \alpha^*}{Re} \int_o^{\pi} (\partial\zeta/\partial\alpha)_o \sin\beta \, d\beta, \tag{108}$$

where the subscripts denote values at $\alpha = 0$. There is a slight inconsistency in this definition of C_D and that used for the circular cylinder. On the basis of (108) the drag values for the circular cylinder should be divided by two to be comparable. The basis used here is chosen to be consistent with the usual definition adopted for a flat plate. The first and second terms on the right side of (108) give respectively the friction drag coefficient C_f and the pressure drag coefficient C_p. Values of the drag coefficients calculated from the solutions are given in Table 4.

Re	C_f	C_p	C_D	A	B	$h=h_1$	α_m/π
1	3.429	0.682	4.111	0.704	0.477	$\pi/20$	1
10	0.756	0.168	0.924	1.957	0.530	$\pi/20$	1
20	0.495	0.119	0.614	2.789	0.482	$\pi/20$	1
40	0.314	0.083	0.397	4.026	0.400	$\pi/30$	1
100	0.184	0.059	0.243	6.782	0.207	$\pi/40$	1
200	0.124	0.046	0.170	10.336	-0.005	$\pi/60$	5/4

TABLE 4. Steady drag on elliptic cylinder

It will be observed that the friction drag contributes the major portion of the total drag over the whole range and still accounts for more than 70% at Re = 200. Only a very minor proportion of the friction drag comes from the region between the leading edge of the cylinder and the peak of the vorticity curve in Figure 18. This can be seen by evaluating the portion of the friction drag integral in (108) between $\phi = 0$ and $\phi = \alpha^*$, making use of the expression (106) for ζ. If it is assumed that α^* is small, the required contribution is found to be approximately,

$$C_f' = \frac{2A\cosh\,\alpha^*}{Re} \int_0^{\alpha^*} \frac{\phi^2 d\phi}{\phi^2 + \alpha^{*2}} \quad .$$

Evaluation of the integral gives

$$C_f' = 2(1-\pi/4)ARe^{-1}\alpha^*\cosh\,\alpha^*$$

and it is then found by calculation from values of A in Table 4 that the contribution of C_f' to the total frictional drag C_f varies from about 1.8% at Re = 1 to 3.7% at Re = 200.

Except for very low Reynolds numbers the frictional drag coefficient in Table 4 agrees reasonably well with the skin friction drag values for a flat plate calculated by Dennis and Dunwoody. The present values are

a little lower. At higher Reynolds there is also remarkable agreement with the formula

$$C_f \sim 1.328Re^{-\frac{1}{2}} + 5.3Re^{-1}$$

suggested by Van Dyke [40] as the correct version of the formula of Kuo [41] for the drag of a flat plate. Thus, apart from the presence of a small pressure drag and the effect of the rounded leading edge, the behavior of the cylinder with regard to drag is essentially similar to that of a flat plate, even for this relatively large thickness to length ratio.

As the Reynolds number becomes larger the flow will eventually separate from the rear of the cylinder. It will first start to separate at $\beta = 0$ for some critical Reynolds number which makes $B = 0$, where

$$B = \sum_{n=1}^{\infty} n r_n(0).$$

Values of B are shown in Table 4. They indicate that separation starts for a Reynolds number between 100 and 200 and, probably, quite close to 200. It may be noted that separation can be predicted with reasonable certainty more or less independently of the grid size used in solving equation (10). The value $\beta = \beta_s$ at the separation point satisfies (99) and depends only on $r_n(0)$, whose calculation involves integration over every grid point in the field of computation and is not dependent on local errors, such as near the body itself. For the solution at Re = 200, the value $\beta_s = 6^o$ is obtained, corresponding to $x^* = 0.9945$. Finally, pressure distributions are given in Figure 19, in which the coefficient (102) is plotted. The curves exhibit strong gradients near the leading edge. The behavior at the trailing edge for Re = 200 indicates that separation has started. The curve Re = 100 is consistent with the rest of the results but has been omitted.

Finally, a check on the numerical solutions is available because of the known result (78). The constant c in this result is determined as part of the computation, but it can also be determined theoretically in terms of the drag coefficient C_D, the required formula being given in the Appendix. The value of C_D is determined by an integration round the cylinder, and this gives an independent estimate of c. The two values should agree, although very high precision cannot be expected because, in effect, the agreement is a test of the balance of inflow and outflow over a very large contour surrounding the cylinder, which is a very stringent criterion. In all the numerical solutions the test was satisfied to an acceptable degree of precision.

DISCUSSION

The practical results given in the previous two sections indicate that satisfactory solutions to the problem of flow past cylinders can be obtained using the numerical technique which has been described. Much of the work of the report has been directed towards the solution of this type of problem. As to the numerical techniques themselves, and their efficiency, a number of points remain to be investigated. No further detailed discussion will be given here, but a few comments can be added regarding certain features of the numerical procedures.

The basic method was designed mainly to dispense with the necessity of solving the Poisson equation (9) as a boundary-value problem. Thus, by utilizing the series (23) for the stream function, it is possible to formulate an approach in which the ordinary differential equations (24) can be solved using step-by-step techniques. The question of whether much reduction in computational labor is achieved has yet to be resolved. In almost all previous numerical investigations of the Navier-Stokes

equations, e.g. in the references cited in the present report, it has been customary to solve (9) by iterative methods. On the whole, iterative methods can be time consuming unless very efficient techniques are used. Compared with methods of this kind, the present method possibly does give a reasonable saving in computer time (an example has been quoted by Dennis and Chang [26], p. 163). However, compared with very efficient methods such as the fast Fourier transform method of Hockney [46] and the direct methods of solution recently considered in a report by Rosser [47], the efficiency of the present method as a numerical technique requires further investigation.

In the numerical results which have been described for flow past a circular cylinder, a method was given for improving the approximation to the vorticity equation (10) by taking into account higher difference corrections to the basic finite-difference approximation (68). The correction obtained by this method was found to be small and the method was not applied to subsequent calculations of the flow past an elliptic cylinder. However, several points in this procedure can be noted. The iterative procedure of repeatedly correcting the solution according to the scheme (98) follows, more or less, the procedure of Fox [29]. Recent publications by Pereyra [48], [49] suggest that this iteration may be too elaborate and that it may not be necessary to carry the iteration (98) beyond the first correction (m = 1). It is not possible to say precisely if this is the case without further investigation, because the present problem is more complicated than that considered by Pereyra. One of the complications is that the boundary condition for ζ on $\alpha = 0$ (i.e. on the line OZ in Figure 3), which enters into the correction K_o on adjacent

grid lines, is itself a function of the corrected solution. The iteration (98) does take account of this.

Finally, in the application we have given of the method of difference correction, only the difference equations (68) which approximate (10) were corrected for the effect of higher differences and not the equations which were used to approximate the differential equations (24). A detailed explanation of the reason for this is lengthy, owing to the specialized technique used to solve (24), but the following is a rough explanation. Equation (68) arises from approximating ζ locally by a polynomial of the second degree and the addition of the difference correction represents, effectively, a system in which ζ is approximated locally by a polynomial of the fourth degree. In the equations which approximate to the differential equations (24), it is more difficult to give a precise analogy because of the specialized method of approximation. However, the right side r_n is approximated locally by a polynomial of the second degree in the formulae which have been used and, roughly, this is already equivalent to approximating f_n by a polynomial of the fourth degree at each grid point. The addition of any further corrections would imply approximation to f_n by a polynomial of even higher degree than the fourth.

APPENDIX

The equations which relate the dimensionless coordinates (x,y), the dimensionless velocity vector $\underset{\sim}{V}$, and the dimensionless pressure p to the corresponding (primed) dimensional quantities are

$$x' = dx,\ y' = dy,\ \underset{\sim}{V}' = U\underset{\sim}{V},\ p' = \rho U^2 p.$$

In these, d is a representative length, U is a representative velocity, and ρ is the density. The generalized Reynolds number R is defined as $R = Ud/\nu$, where ν is the coefficient of kinematical viscosity. The time t is related to the actual time, t', by $t = Ut'/d$.

Let (u,v) be the dimensionless components of the velocity vector $\underset{\sim}{V}$ in the directions of increase of the coordinates (α,β). The components are related to the stream function by the equations

$$u = H\frac{\partial\psi}{\partial\beta},\quad v = -H\frac{\partial\psi}{\partial\alpha}. \tag{A.1}$$

The dimensionless vorticity vector is $\underset{\sim}{\omega} = \text{curl}\ \underset{\sim}{V} = (0,0,-\zeta)$, where

$$\zeta = H^2\{\frac{\partial}{\partial\beta}(\frac{u}{H}) - \frac{\partial}{\partial\alpha}(\frac{v}{H})\}. \tag{A.2}$$

Equations (A.1) and (A.2) give rise to equation (9). The equations of motion of an incompressible fluid can be written (see Goldstein [42]) as

$$\partial\underset{\sim}{V}/\partial t - \underset{\sim}{V} \times \underset{\sim}{\omega} = -\ \text{grad}(p+\tfrac{1}{2}V^2) - R^{-1}\text{curl}\ \underset{\sim}{\omega}. \tag{A.3}$$

The equation (10) for the component ζ can be obtained by taking the curl of (A.3). When separated into components, the first two equations are identically zero and the third gives (10).

The pressure distribution over the cylinder is obtained from (A.3). If we take the component equation in the β-direction on the cylinder, where $u = v = 0$, then on $\alpha = 0$

$$\frac{\partial p}{\partial\beta} = -R^{-1}\frac{\partial\zeta}{\partial\alpha} \tag{A.4}$$

and hence

$$p(\beta,t) - p_o(t) = -R^{-1} \int_{\beta_o}^{\beta} (\frac{\partial \zeta}{\partial \alpha})_{\alpha=0} d\beta, \qquad (A.5)$$

where p_o is the pressure at some base point $\beta = \beta_o$ on the cylinder. This can be obtained in terms of the uniform pressure p_∞ at large distance from the cylinder by integrating the component equation of (A.3) in the α-direction along $\beta = \beta_o$. This component equation can be written

$$\frac{\partial}{\partial \alpha} (p+\tfrac{1}{2}V^2) = R^{-1} \frac{\partial \zeta}{\partial \beta} + \zeta \frac{\partial \psi}{\partial \alpha} - H^{-1} \frac{\partial u}{\partial t}$$

and hence

$$p_o - p_\infty = \tfrac{1}{2} - \int_o^\infty (R^{-1} \frac{\partial \zeta}{\partial \beta} + \zeta \frac{\partial \psi}{\partial \alpha} - H^{-1} \frac{\partial u}{\partial t}) d\alpha, \qquad (A.6)$$

where the path of integration $\beta = \beta_o$ is understood in the integral.

Pressure variations are usually exhibited in terms of the pressure coefficient $P(\beta,t)$ defined by

$$P(\beta,t) = \frac{p'(\beta,t) - p'_\infty}{\tfrac{1}{2}\rho U^2} = 2\{p(\beta,t) - p_\infty\}, \qquad (A.7)$$

which is obtained by addition of (A.5) to (A.6). The only pressure calculations carried out in the present report are for steady flow and in this case the steady pressure coefficient $P(\beta)$ is

$$P(\beta) = 1 - 2R^{-1} \int_{\beta_o}^{\beta} (\frac{\partial \zeta}{\partial \alpha})_{\alpha=0} d\beta - 2 \int_o^\infty (R^{-1} \frac{\partial \zeta}{\partial \beta} + \zeta \frac{\partial \psi}{\partial \alpha})_{\beta=\beta_o} d\alpha. \qquad (A.8)$$

In the case of flow past a circular cylinder it is convenient to take $\beta_o = \pi$, in which case the second term in the second integral in (A.8) is zero. For the elliptic cylinder the path $\beta_o = \pi/2$ was chosen. Essentially, the reason for the change is that $\partial\zeta/\partial\beta$ in the integral in (A.6) varies rapidly near the leading edge of the ellipse (it is infinite for the limiting case $\alpha^* = 0$ of a flat plate) and may lead to an inaccurate value of p_o.

The drag D exerted by the fluid on the cylinder is given by

$$D = -\rho U \int_C (\nu\zeta\, dx + dUp\, dy),$$

where all quantities in the right side are the dimensionless quantities already defined. Integration is round the contour C of the cylinder ($\alpha = 0$) in the anti-clockwise sense. The first and second parts of the integral give respectively the friction drag and the pressure drag. The second integral can be expressed more conveniently by integrating by parts and making use of (A.4). Then

$$D = -\rho U \int_C \left[\nu\zeta \left(\frac{\partial x}{\partial \beta}\right)_{\alpha=0} + UdR^{-1}y\left(\frac{\partial \zeta}{\partial \alpha}\right)_{\alpha=0}\right] d\beta. \qquad (A.9)$$

The drag coefficient C_D is defined as $D/\rho U^2 b$, where b is some dimension of the cylinder. For a circular cylinder b is usually taken as the radius, while for a flat plate it is taken as the length of the plate.

The constant c in (78) can be expressed in terms of C_D in a manner similar to that considered in Ref. [12]. As $\alpha \to \infty$, the expression for ψ which corresponds to (78) is

$$\psi \sim ke^{\alpha}\sin\beta - \tfrac{1}{2}\pi c(1-\beta/\pi), \qquad (A.10)$$

except at $\beta = 0$, where a finite discontinuity exists. Goldstein [43] has shown that the drag on the cylinder can be expressed by the formula

$$D = \rho UI, \qquad (A.11)$$

where I is the inflow in the wake over a large contour surrounding the cylinder. As $\alpha \to \infty$, the wake coincides with $\beta = 0$ and the inflow is found as the total increase in ψ' in going once round the large contour from $\beta = 0$ to $\beta = 2\pi$, where ψ' is the dimensional stream function, viz. $\psi' = Ud\psi$. Thus, from (A.10),

$$I = \pi cUd,$$

and if, as above, we take $C_D = D/\rho U^2 b$, then from (A.11) we obtain

$$c = bC_D/\pi d. \qquad (A.12)$$

The expression (A.12) allows a check on the numerical solutions. The coefficient $\frac{1}{2}\pi c$ which appears in (A.10) is consistent with the value $\frac{1}{2}C_D$ used by Kawaguti [44] in the condition at infinity appropriate to the flow past a circular cylinder. For the flat plate considered in Ref. [12], the appropriate value of $\frac{1}{2}\pi c$ is C_D, because of the different definition of C_D.

Finally, only symmetrical flow past cylinders is considered in the present report. Any type of asymmetry is ruled out by the basic assumptions. Thus, no reference is made to the numerous investigations of unsteady asymmetrical motion past cylinders, such as those which attempt to predict the vortex street behind the cylinder.

As to the results (mentioned in the footnote on p. 48) given by Hamielec and Raal [45] for steady flow past a circular cylinder, the one calculation beyond Re = 50* which can be compared with present results is that for Re = 100. Their value of $\beta_s = 66.8^o$ for the separation angle is in good agreement with present results, but the estimated values of $C_D = 1.172$ and $L = 9.48$ differ considerably from those of the present report. Hamielec and Raal obtain several solutions for each Reynolds number with different positions of the outer boundary $\alpha = \alpha_m$. The greatest value of α_m for Re = 100 corresponds to a distance of only 12.2 radii from the center of the cylinder. This seems to be too close to the cylinder; according to present results it would actually be within the region of the recirculating wake.

---

* It may be recalled that for a circular cylinder the Reynolds number Re is that based on the diameter of the cylinder and, in this case, is twice the generalized Reynolds number R used elsewhere in this Appendix.

REFERENCES

1. D. Greenspan, P.C. Jain, R. Manohar, B. Noble and A. Sakurai, Mathematics Research Center, Technical Summary Report No. 482, Madison, 1964.

2. M. Kawaguti, J. Phys. Soc. Japan 16 (1961), 2307.

3. L.M. Simuni, Inzhenernii Zhournal (USSR) 4 (1964), 446.

4. R.D. Mills, J. Roy. Aero. Soc. 69 (1965), 714.

5. O.R. Burggraf, J. Fluid Mech. 24 (1966), 113.

6. F. Zabransky. Numerical solutions for fluid flow in rectangular cavities. Ph.D. Thesis, University of Western Ontario, 1968.

7. R.B. Payne, J. Fluid Mech. 4 (1958), 81.

8. M. Kawaguti and P. Jain, Mathematics Research Center, Technical Summary Report No. 590, Madison, 1965.

9. C.J. Apelt, Aeronautical Research Council Reports and Memoranda No. 3175, London, 1961.

10. H.B. Keller and H. Takami. Numerical solution of nonlinear differential equations (D. Greenspan, Ed.), John Wiley and Sons, New York, 1966, p. 115.

11. E. Janssen, J. Fluid Mech. 3 (1957), 329.

12. S.C.R. Dennis and J. Dunwoody, J. Fluid Mech. 24 (1966), 577.

13. L. Fox. The numerical solution of two-point boundary problems in ordinary differential equations. Clarendon Press, Oxford, 1957, p. 18.

14. H. Jeffreys and B.S. Jeffreys. Methods of Mathematical Physics. 3rd edn. Cambridge University Press, 1962, p. 441.

15. L.N.G. Filon, Proc. Roy. Soc. Edin. 49 (1928), 38.

16. G.E. Forsythe and W.R. Wasow. Finite-difference methods for partial differential equations. John Wiley and Sons, New York, 1960, p. 30.

17. J.F. Steffensen. Interpolation. The Williams and Wilkins Company Baltimore, 1927.

18. A. Thom and C.J. Apelt, Aeronautical Research Council Reports and Memoranda No. 3061, London, 1958.

19. D. Greenspan in Lectures on the numerical solution of linear, singular, and nonlinear differential equations. Prentice-Hall, New Jersey, 1968, Chap. 10.

20. H. Lamb. Hydrodynamics. 6th Ed. Cambridge University Press, 1932, p. 609.

21. S.C.R. Dennis, J.D. Hudson and N. Smith, Phys. Fluids 11 (1968), 933.

22. I. Imai, Proc. Roy. Soc. A 208 (1951), 487.

23. H. Schlichting. Boundary layer theory. 4th Ed. McGraw-Hill, New York, 1960.

24. D.B. Ingham, J. Fluid Mech. 31 (1968), 815.

25. S. Goldstein and L. Rosenhead, Proc. Camb. Phil. Soc. 32 (1936), 392.

26. S.C.R. Dennis and G.Z. Chang. Proceedings of the U.S. Army Numerical Analysis Conference, Fort Monmouth, New Jersey, 1968, p.117.

27. J.S. Son and T.J. Hanratty, J. Fluid Mech. 35 (1969), 369.

28. H. Takami and H.B. Keller, Phys. Fluids (to be published).

29. L. Fox, Proc. Roy. Soc. A 190 (1947), 31.

30. D.N. de G. Allen and R.V. Southwell, Quart. J. Mech. Appl. Math. 8 (1955), 129.

31. S.C.R. Dennis and M. Shimshoni, Aeronautical Research Council Current Papers No. 797, London, 1965.

32. S. Taneda, J. Phys. Soc. Japan 11 (1956), 302.

33. A. Acrivos, L.G. Leal, D.D. Snowden and F. Pan, J. Fluid Mech. 34 (1968), 25.

34. D.J. Tritton, J. Fluid Mech. 6 (1959), 547.

35. I. Imai, University of Maryland Tech. Note No. BN-104, 1957.

36. S. Brodetsky, Proc. Roy. Soc. A102 (1923), 542.

37. A. Roshko, Proceedings of the Canadian Congress of Applied Mechanics, Vol. 3, 1967, p. 81.

38. V.V. Sychev, Symposium on Modern Problems in Fluid and Gas Dynamics Tarda, Poland, 1967.

39. A. Acrivos, D.D. Snowden, A.S. Grove and E.E. Petersen, J. Fluid Mech. 21 (1965), 737.

40. M. Van Dyke, J. Fluid Mech. 14 (1962), 481.

41. Y.H. Kuo, J. Math. Phys. 32 (1953), 83.

42. S. Goldstein (Editor). Modern Developments in Fluid Dynamics. Clarendon Press, Oxford, 1938, Vol. I, p. 100.

43. S. Goldstein, Proc. Roy. Soc. A 123 (1929), 216.

44. M. Kawaguti, J. Phys. Soc. Japan 8 (1953), 747.

45. A.E. Hamielec and J.D. Raal, Phys. Fluids 12 (1969), 11.

46. R.W. Hockney, J. Assoc. Comp. Machinery 12 (1965), 95.

47. J.B. Rosser, Mathematics Research Center, Technical Summary Report No. 797, Madison, 1967.

48. V. Pereyra, Mathematics Research Center, Technical Summary Report No. 687, Madison, 1966.

49. V. Pereyra, SIAM J. Numer. Anal. 4, (1967), 508.

FIGURE 1 Flow in rectangular cavity.

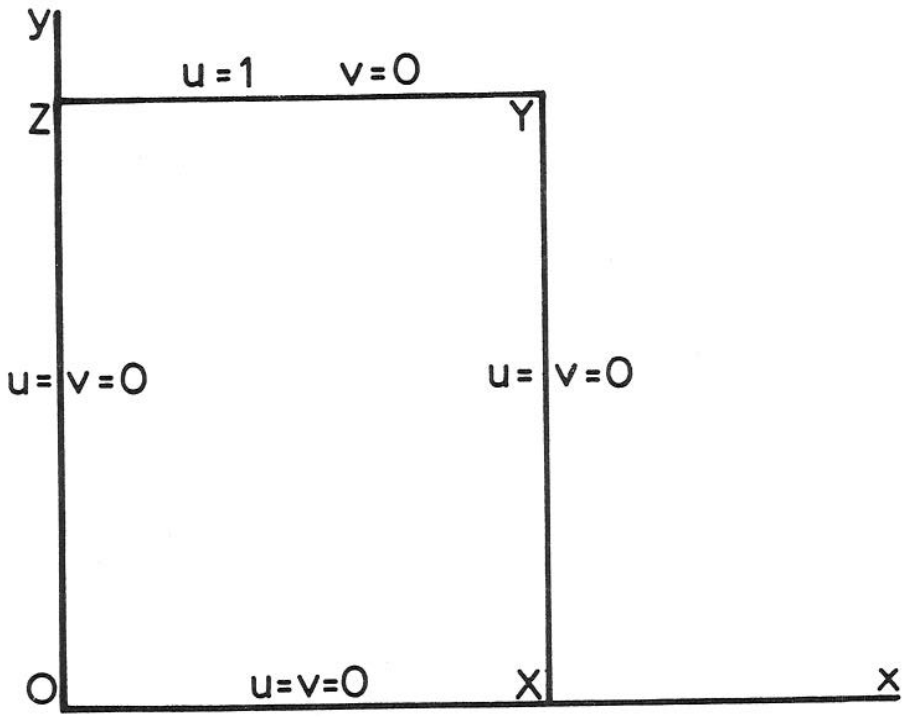

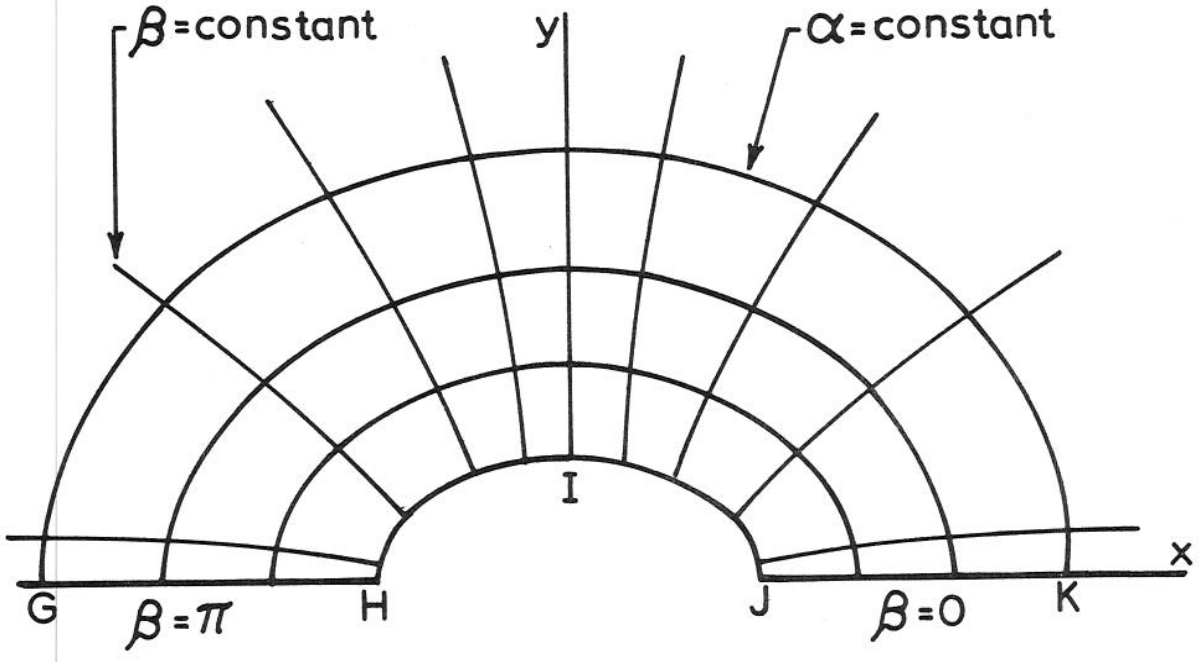

FIGURE 2 Curvilinear coordinates (α,β).

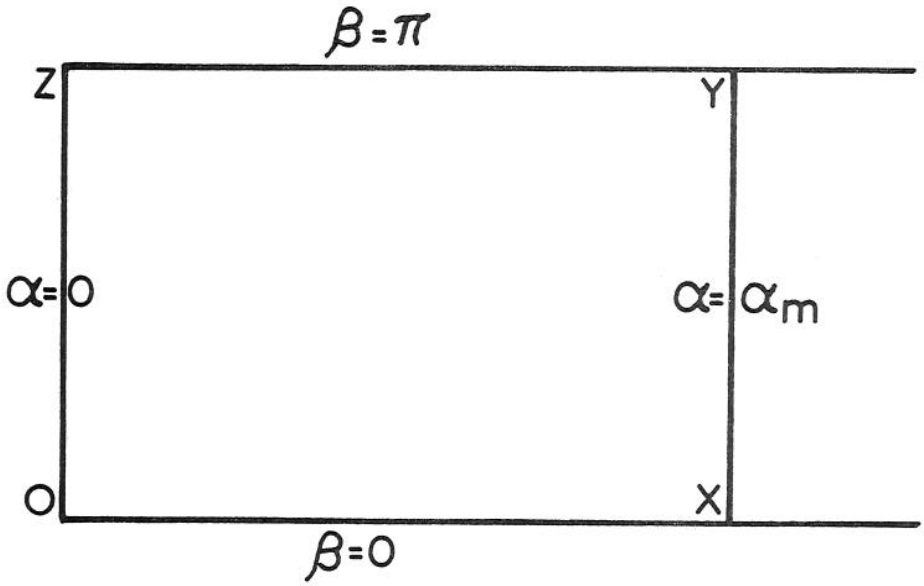

FIGURE 3 Transformed domain of integration.

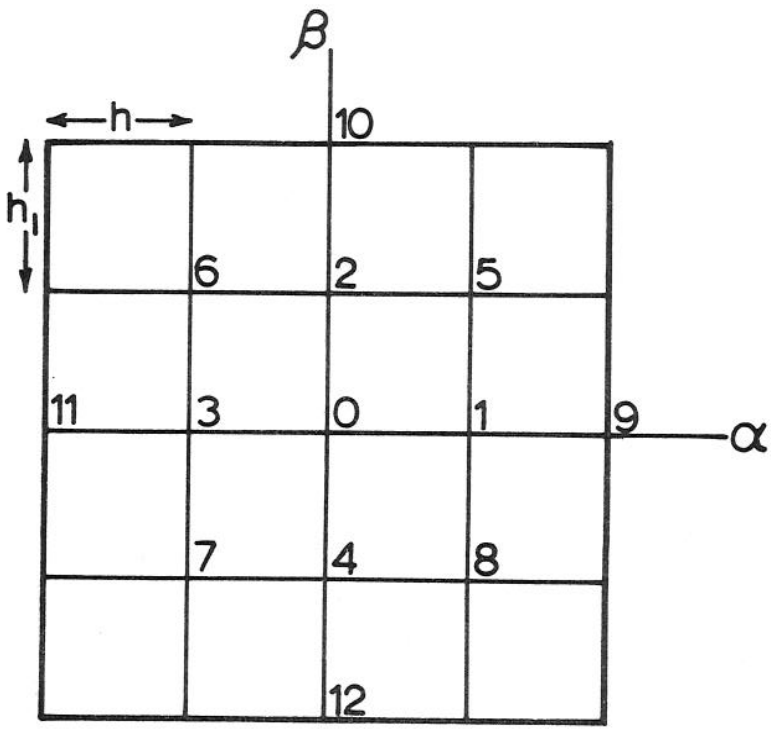

FIGURE 4 Numbering system for grid points.

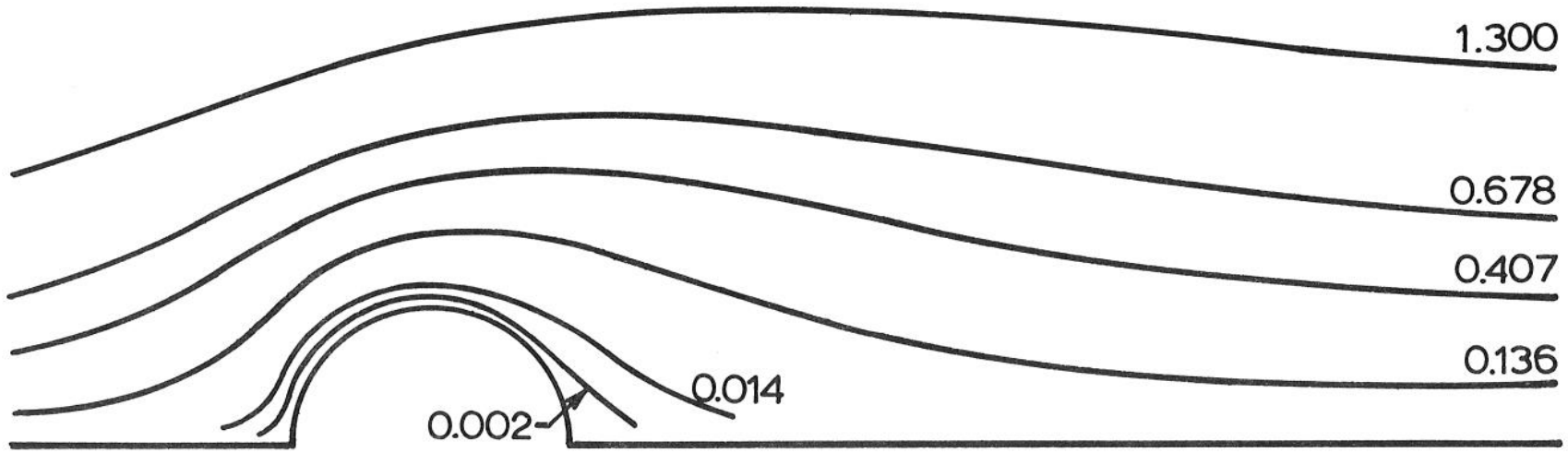

FIGURE 5 Streamlines for Re = 5. Values of the dimensionless stream function, ψ, are shown for each streamline. Re is the Reynolds number based on the diameter.

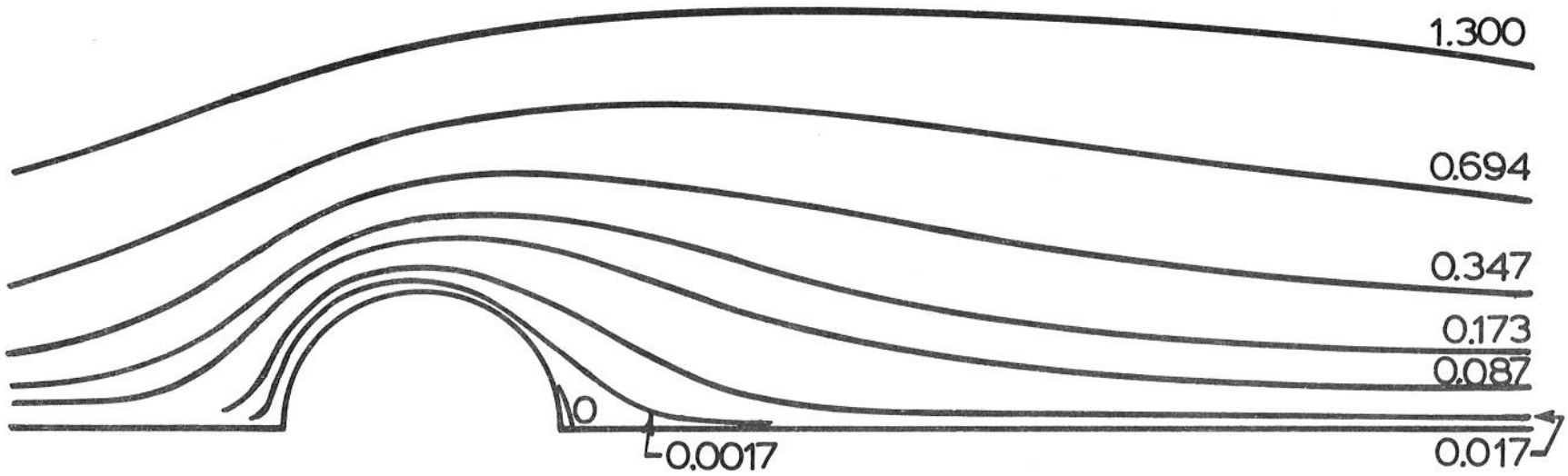

FIGURE 6 Streamlines for Re = 7.

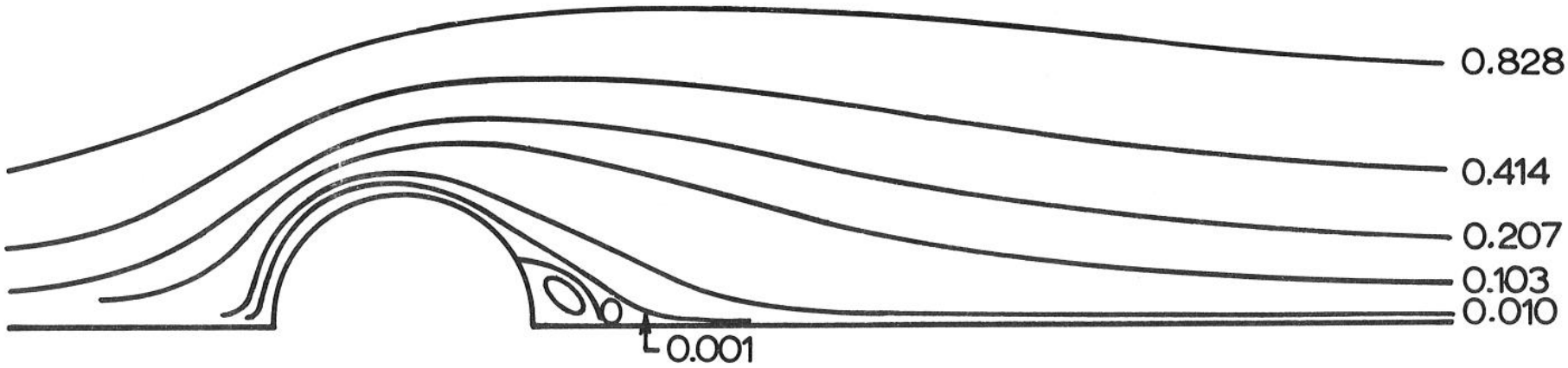

FIGURE 7 Streamlines for Re = 10. The closed streamline corresponds to $\psi = -0.0002$.

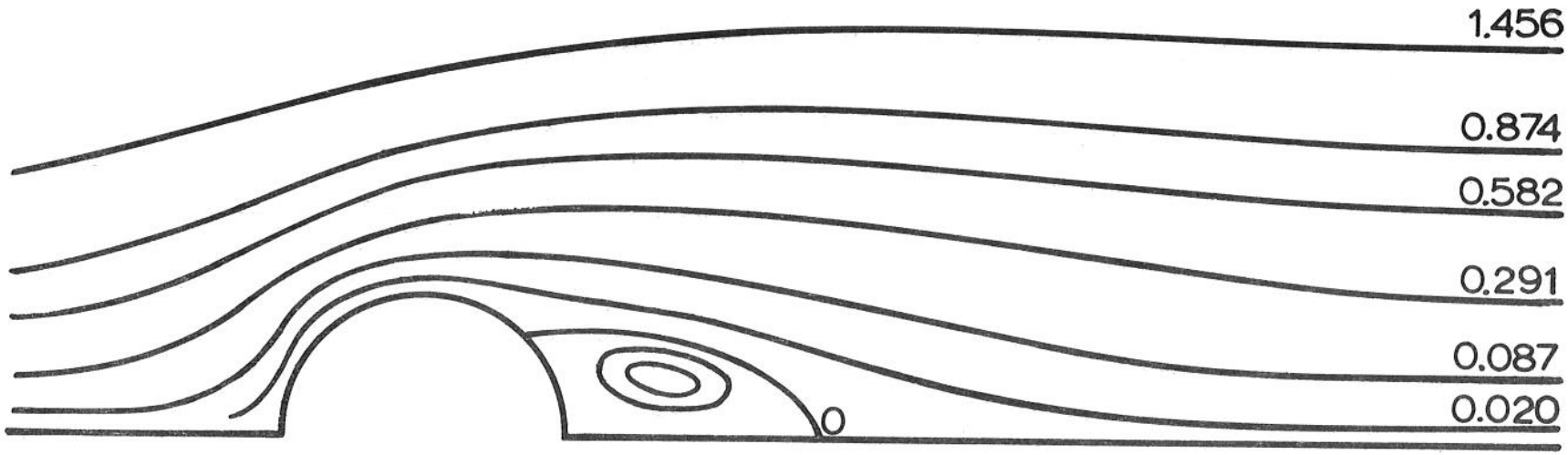

FIGURE 8 Streamlines for Re = 20. The closed streamlines, starting from the center, correspond to ψ = -0.008, -0.0058.

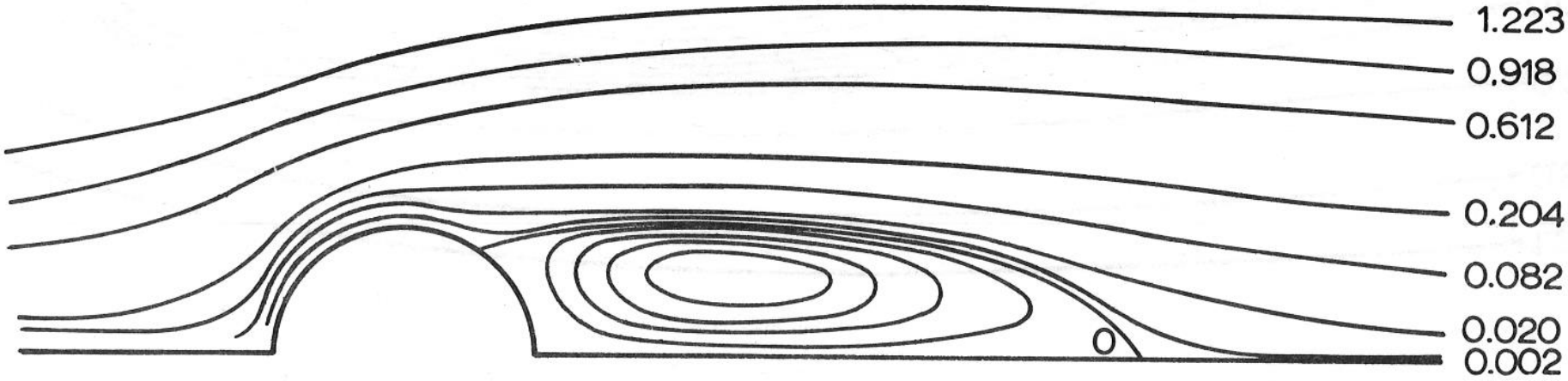

FIGURE 9 Streamlines for Re = 40. The closed streamlines, starting from the center, correspond to ψ = -0.0328, -0.0246, -0.0164, -0.0082.

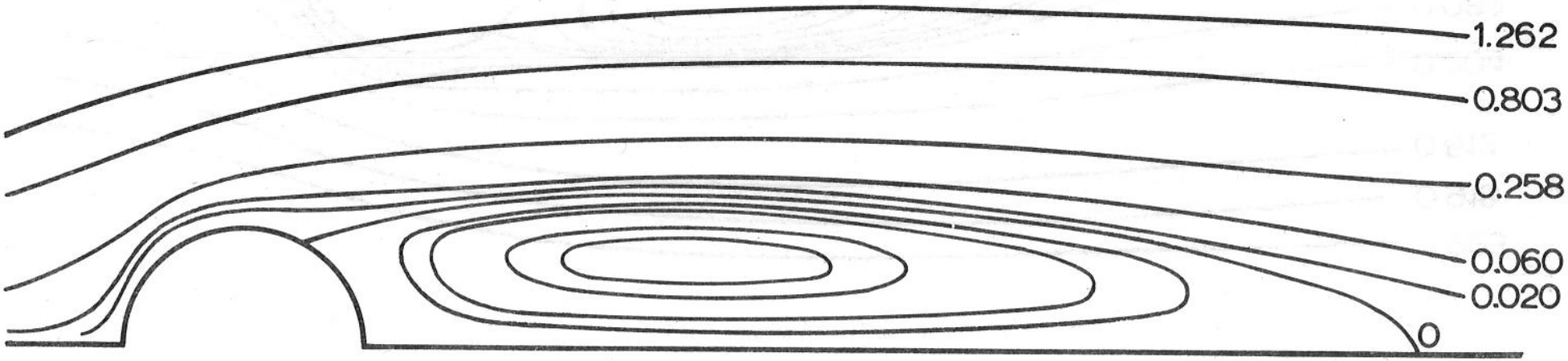

FIGURE 10 Streamlines for Re = 70. The closed streamlines, starting from the center, correspond to ψ = -0.07, -0.06, -0.035, -0.023.

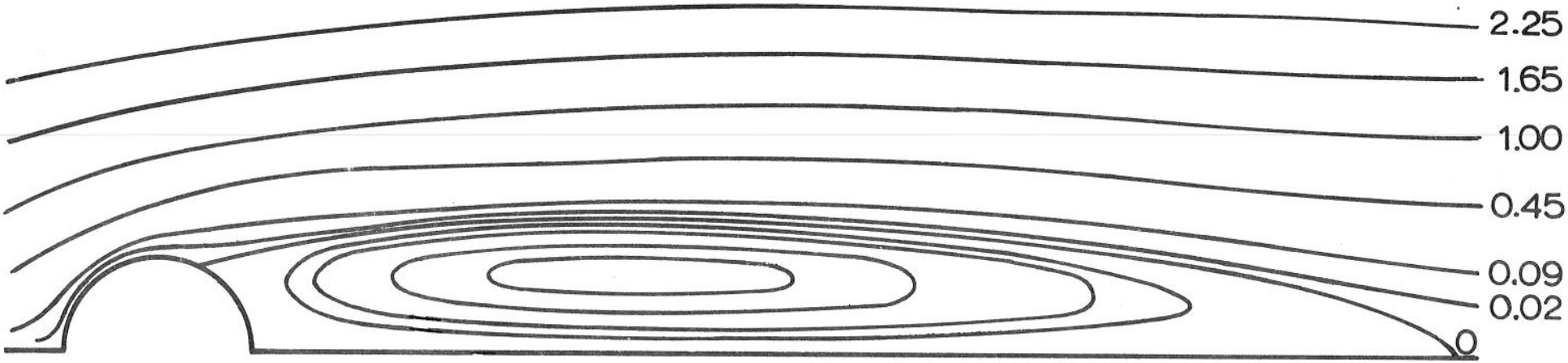

FIGURE 11 Streamlines for Re = 100. The closed streamlines, starting from the center, correspond to ψ = -0.1, -0.08, -0.05, -0.035.

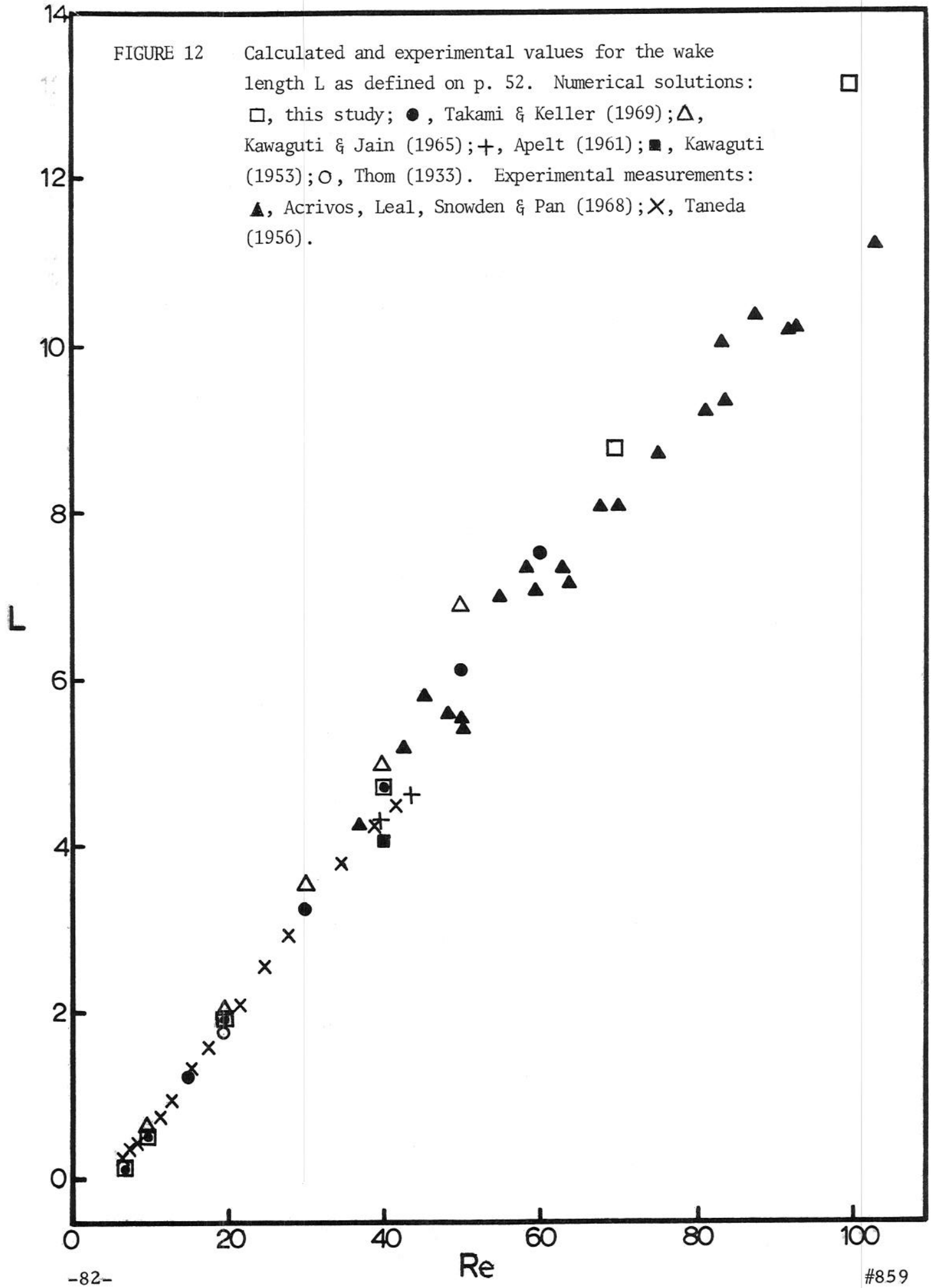

FIGURE 12 Calculated and experimental values for the wake length L as defined on p. 52. Numerical solutions: □, this study; ●, Takami & Keller (1969); △, Kawaguti & Jain (1965); +, Apelt (1961); ■, Kawaguti (1953); ○, Thom (1933). Experimental measurements: ▲, Acrivos, Leal, Snowden & Pan (1968); ×, Taneda (1956).

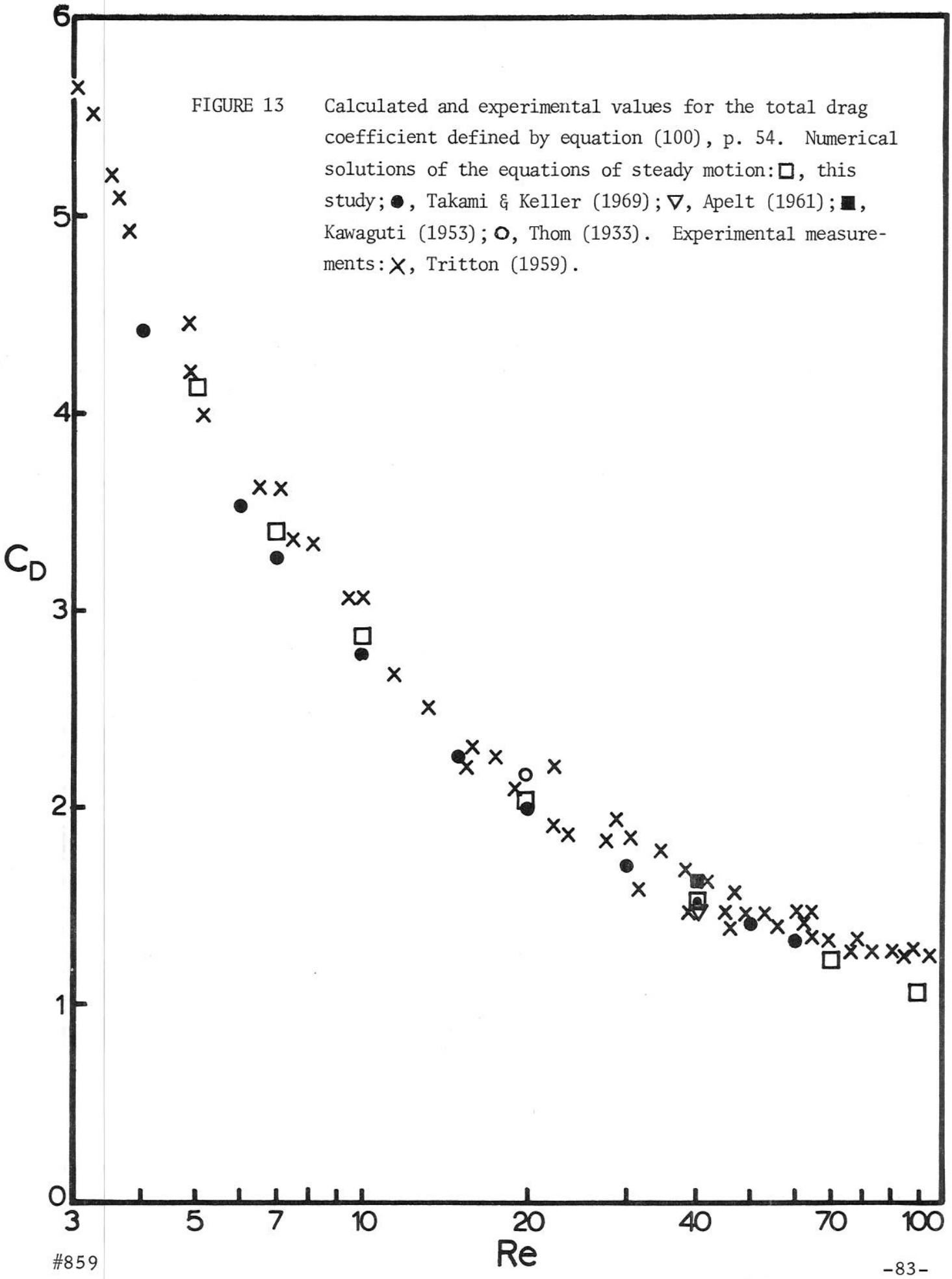

FIGURE 13 Calculated and experimental values for the total drag coefficient defined by equation (100), p. 54. Numerical solutions of the equations of steady motion: □, this study; ●, Takami & Keller (1969); ▽, Apelt (1961); ■, Kawaguti (1953); ○, Thom (1933). Experimental measurements: ×, Tritton (1959).

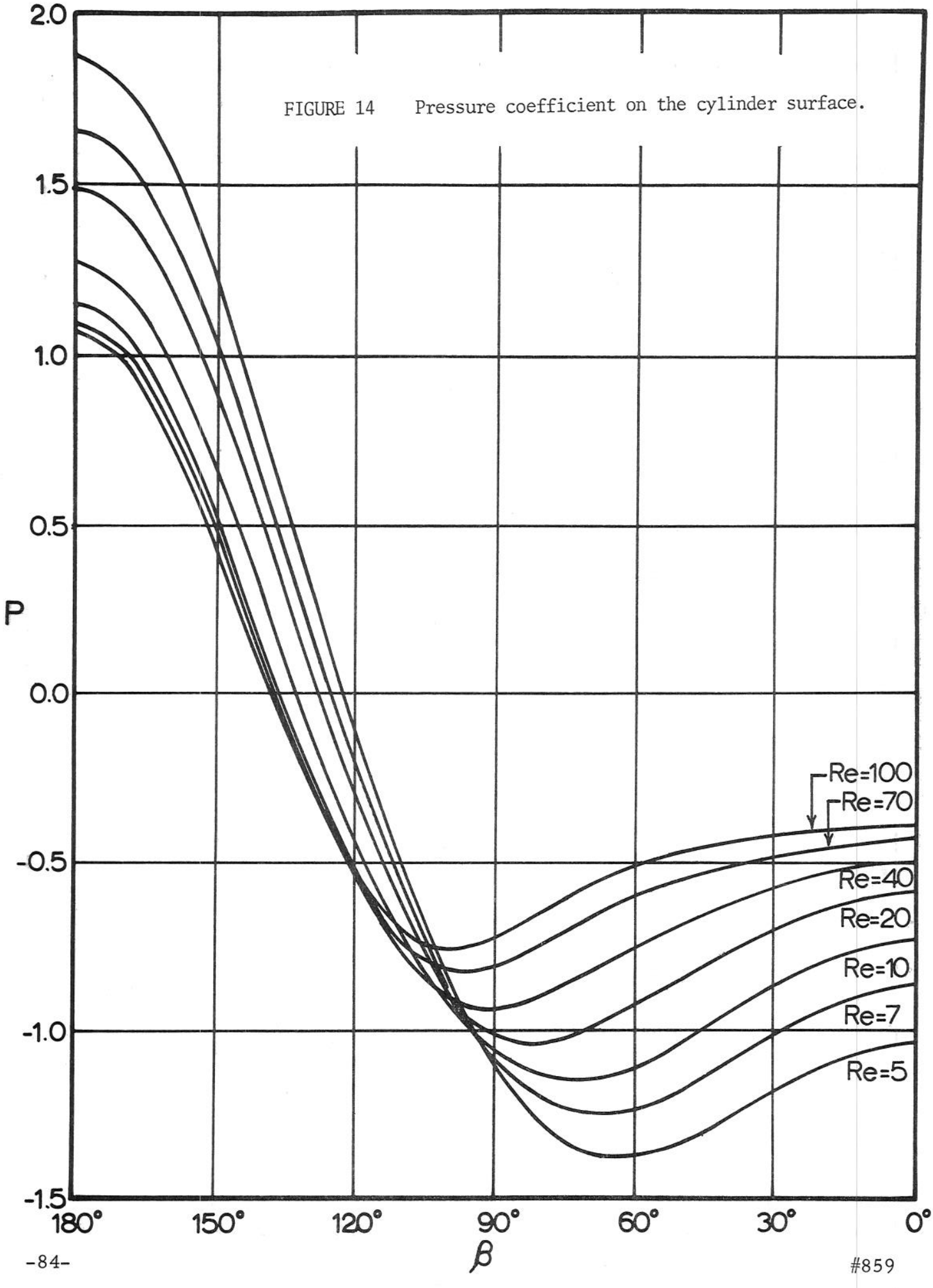

FIGURE 14 Pressure coefficient on the cylinder surface.

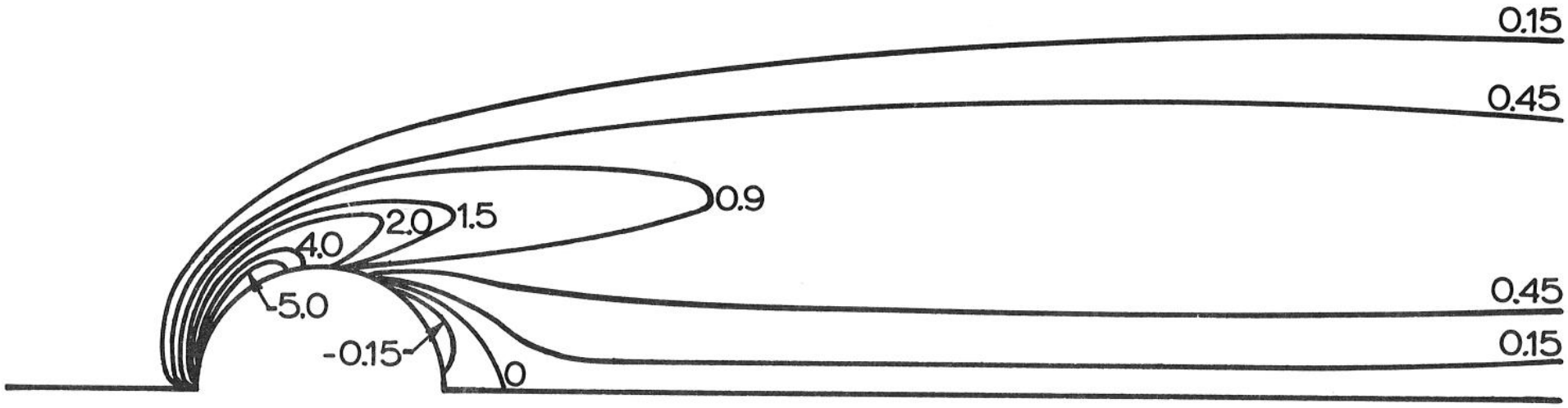

FIGURE 15 Equi-vorticity lines for Re = 70. Values of the negative dimensionless vorticity, ζ, are shown for each equi-vorticity line.

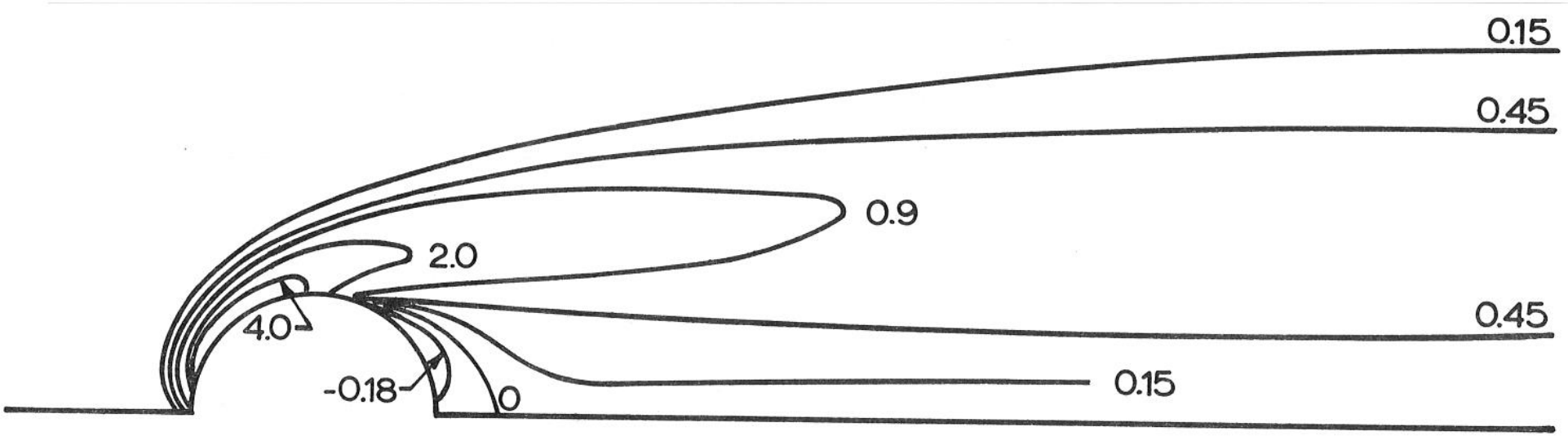

FIGURE 16 Equi-vorticity lines for Re = 100.

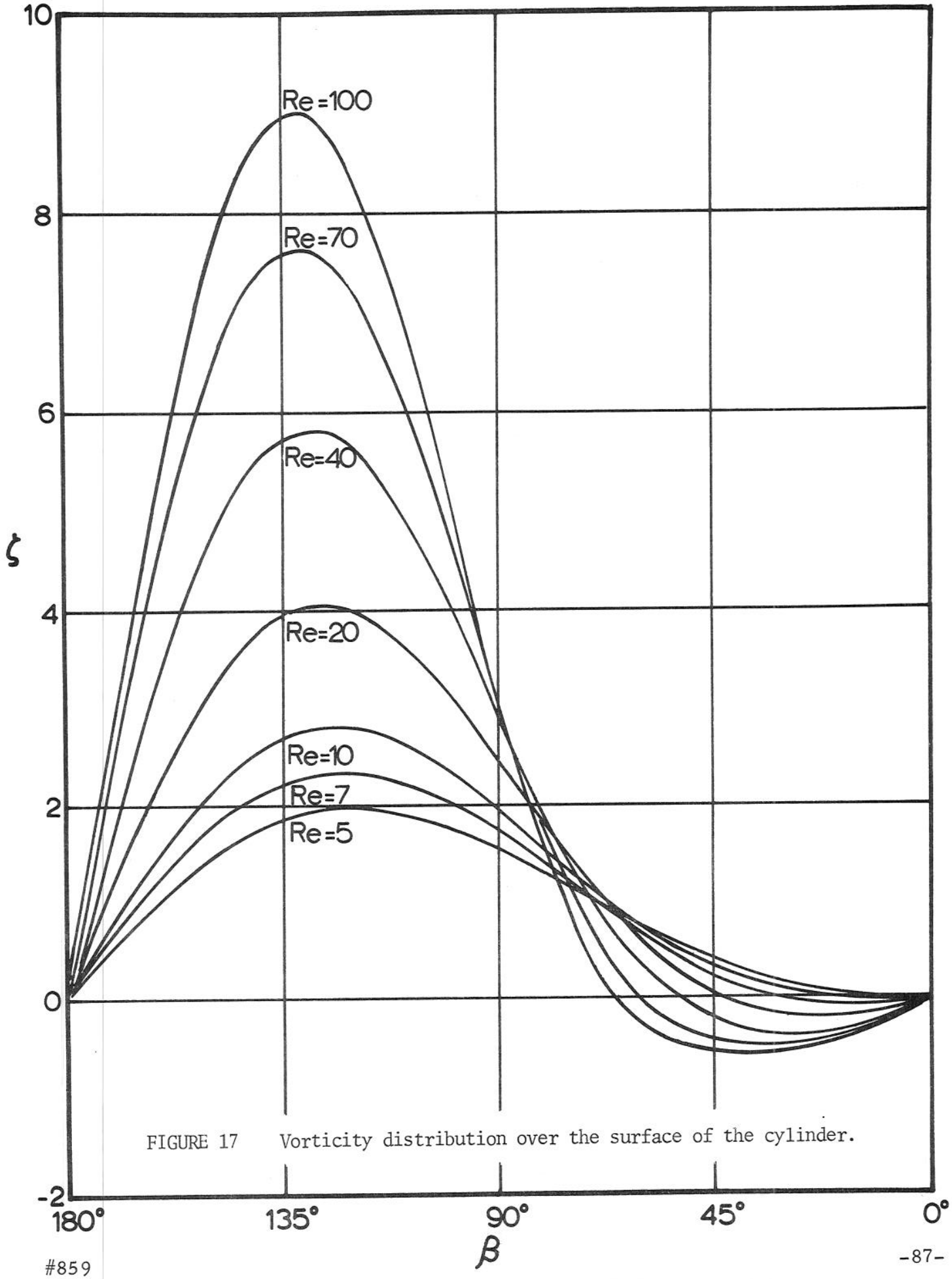

FIGURE 17 Vorticity distribution over the surface of the cylinder.

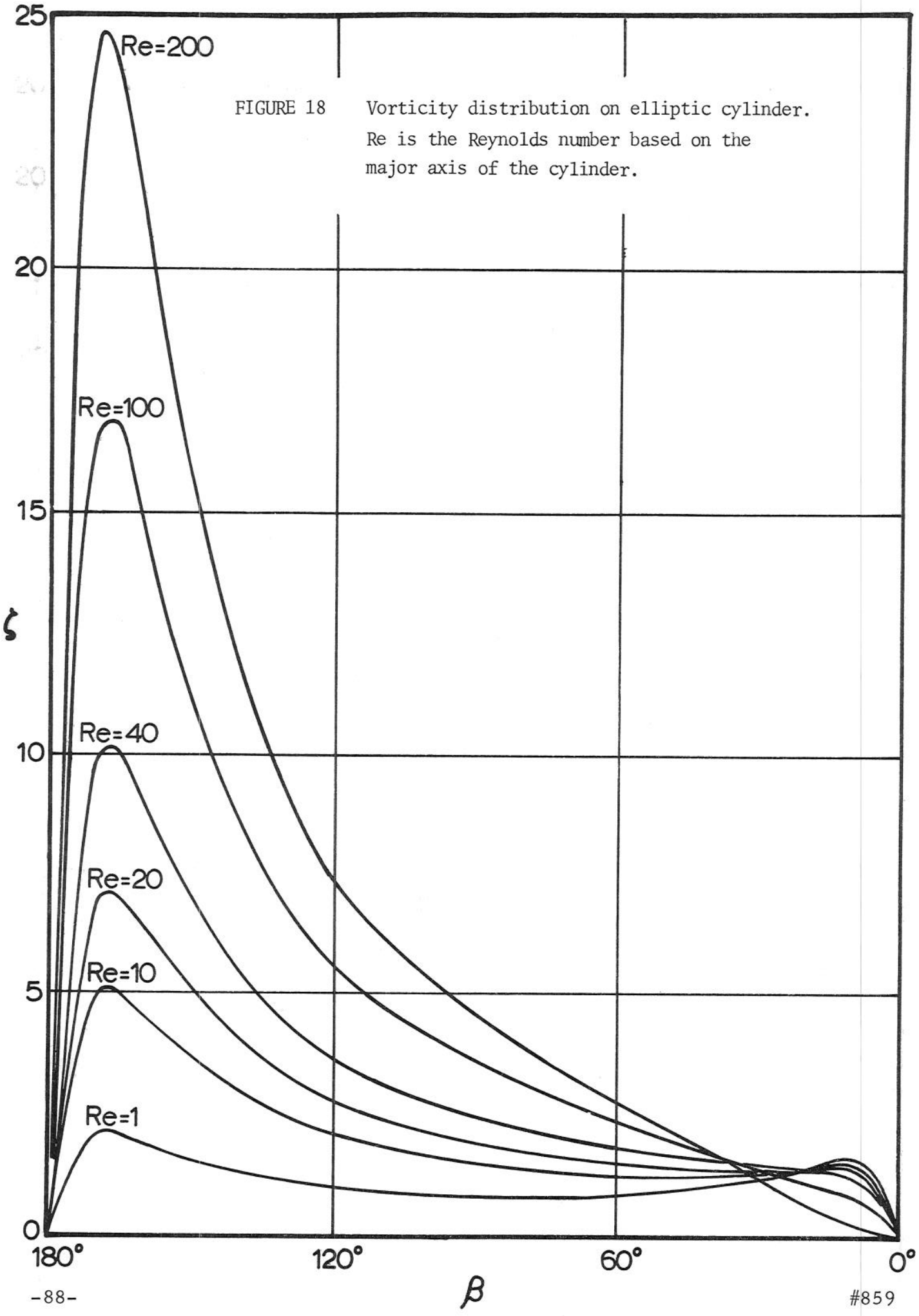

FIGURE 18 Vorticity distribution on elliptic cylinder. Re is the Reynolds number based on the major axis of the cylinder.

FIGURE 19 Pressure coefficient on elliptic cylinder as a function of $x^* = \cos\beta$.

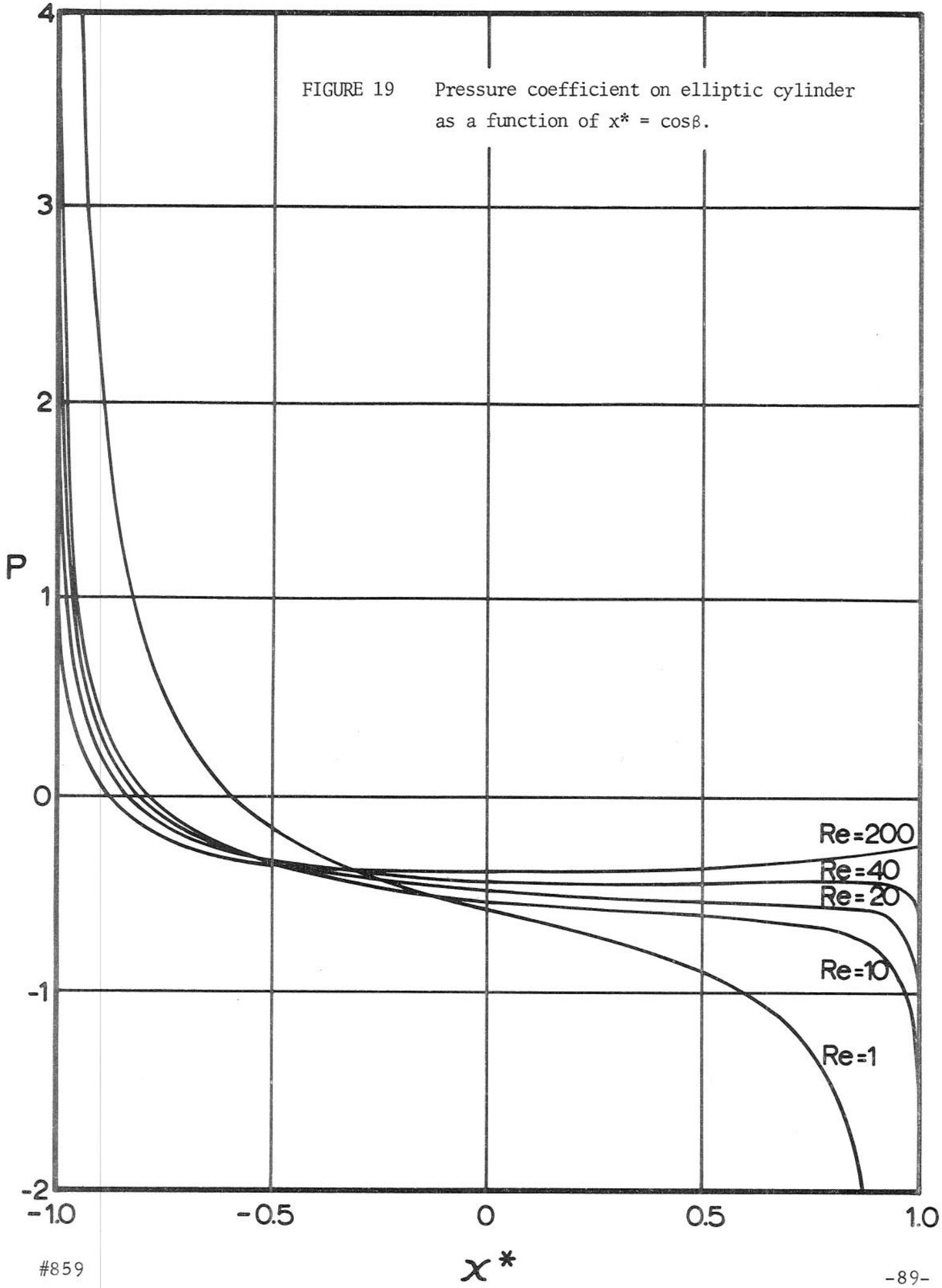

AR 70-31 Unclassified

Security Classification

DOCUMENT CONTROL DATA - R & D

(Security classification of title, body of abstract and indexing annotation must be entered when the overall report is classified)

1. ORIGINATING ACTIVITY (Corporate author)	2a. REPORT SECURITY CLASSIFICATION
Mathematics Research Center, U. S. Army University of Wisconsin, Madison, Wis. 53706	Unclassified
	2b. GROUP None

3. REPORT TITLE

NUMERICAL INTEGRATION OF THE NAVIER-STOKES EQUATIONS IN TWO DIMENSIONS

4. DESCRIPTIVE NOTES (Type of report and inclusive dates)

Summary Report: no specific reporting period.

5. AUTHOR(S) (First name, middle initial, last name)

S. C. R. Dennis and Gau-Zu Chang

6. REPORT DATE	7a. TOTAL NO. OF PAGES	7b. NO. OF REFS
March 1968	89	49

8a. CONTRACT OR GRANT NO.	9a. ORIGINATOR'S REPORT NUMBER(S)
Contract No. DA-31-124-ARO-D-462	859
b. PROJECT NO. None	
c.	9b. OTHER REPORT NO(S) (Any other numbers that may be assigned this report)
d.	None

10. DISTRIBUTION STATEMENT

Distribution of this document is unlimited.

11. SUPPLEMENTARY NOTES	12. SPONSORING MILITARY ACTIVITY
None	Army Research Office-Durham, N.C.

13. ABSTRACT

A numerical method is described for solving the two-dimensional Navier-Stokes equations. Results for steady flow past a circular cylinder for Reynolds numbers up to 100, and past an elliptic cylinder for Reynolds numbers up to 200, are given.

DD FORM 1 NOV 68 1473

Unclassified

Security Classification

AGO 5698A

Mathematics Research Center, U.S.Army | UNCLASSIFIED
NUMERICAL INTEGRATION OF THE NAVIER-STOKES EQUATIONS IN TWO DIMENSIONS

Fluid dynamics

S. C. R. Dennis and Gau-Zu Chang

MRC Report No. 859 AD________ July 1969
Contract No.: DA-31-124-ARO-D-462 89 pp.

A numerical method is described for solving the two-dimensional Navier-Stokes equations. Results for steady flow past a circular cylinder for Reynolds numbers up to 100, and past an elliptic cylinder for Reynolds numbers up to 200, are given.

Mathematics Research Center, U.S.Army | UNCLASSIFIED
NUMERICAL INTEGRATION OF THE NAVIER-STOKES EQUATIONS IN TWO DIMENSIONS

Fluid dynamics

S. C. R. Dennis and Gau-Zu Chang

MRC Report No. 859 AD________ July 1969
Contract No.: DA-31-124-ARO-D-462 89 pp.

A numerical method is described for solving the two-dimensional Navier-Stokes equations. Results for steady flow past a circular cylinder for Reynolds numbers up to 100, and past an elliptic cylinder for Reynolds numbers up to 200, are given.

Mathematics Research Center, U.S.Army | UNCLASSIFIED
NUMERICAL INTEGRATION OF THE NAVIER-STOKES EQUATIONS IN TWO DIMENSIONS

Fluid dynamics

S. C. R. Dennis and Gau-Zu Chang

MRC Report No. 859 AD________ July 1969
Contract No.: DA-31-124-ARO-D-462 89 pp.

A numerical method is described for solving the two-dimensional Navier-Stokes equations. Results for steady flow past a circular cylinder for Reynolds numbers up to 100, and past an elliptic cylinder for Reynolds numbers up to 200, are given.

Mathematics Research Center, U.S.Army | UNCLASSIFIED
NUMERICAL INTEGRATION OF THE NAVIER-STOKES EQUATIONS IN TWO DIMENSIONS

Fluid dynamics

S. C. R. Dennis and Gau-Zu Chang

MRC Report No. 859 AD________ July 1969
Contract No.: DA-31-124-ARO-D-462 89 pp.

A numerical method is described for solving the two-dimensional Navier-Stokes equations. Results for steady flow past a circular cylinder for Reynolds numbers up to 100, and past an elliptic cylinder for Reynolds numbers up to 200, are given.

Mathematics Research Center, U.S.Army UNCLASSIFIED

NUMERICAL INTEGRATION OF THE NAVIER-STOKES EQUATIONS IN TWO DIMENSIONS

S.C.R. Dennis and Gau-Zu Chang

Fluid dynamics

MRC Report No. 859 AD_____ July 1969
Contract No. : DA-31-124-ARO-D-462 89 pp.

A numerical method is described for solving the two-dimensional Navier-Stokes equations. Results for steady flow past a circular cylinder for Reynolds numbers up to 100, and past an elliptic cylinder for Reynolds numbers up to 200, are given.

Mathematics Research Center, U.S.Army UNCLASSIFIED

NUMERICAL INTEGRATION OF THE NAVIER-STOKES EQUATIONS IN TWO DIMENSIONS

S.C.R. Dennis and Gau-Zu Chang

Fluid dynamics

MRC Report No. 859 AD_____ July 1969
Contract No.: DA-31-124-ARO-D-462 89 pp.

A numerical method is described for solving the two-dimensional Navier-Stokes equations. Results for steady flow past a circular cylinder for Reynolds numbers up to 100, and past an elliptic cylinder for Reynolds numbers up to 200, are given.

Mathematics Research Center, U.S.Army UNCLASSIFIED

NUMERICAL INTEGRATION OF THE NAVIER-STOKES EQUATIONS IN TWO DIMENSIONS

S.C.R. Dennis and Gau-Zu Chang

Fluid dynamics

MRC Report No. 859 AD_____ July 1969
Contract No.: DA-31-124-ARO-D-462 89 pp.

A numerical method is described for solving the two-dimensional Navier-Stokes equations. Results for steady flow past a circular cylinder for Reynolds numbers up to 100, and past an elliptic cylinder for Reynolds numbers up to 200, are given.

Mathematics Research Center, U.S.Army UNCLASSIFIED

NUMERICAL INTEGRATION OF THE NAVIER-STOKES EQUATIONS IN TWO DIMENSIONS

S.C.R. Dennis and Gau-Zu Chang

Fluid dynamics

MRC Report No. 859 AD_____ July 1969
Contract No.: DA-31-124-ARO-D-462 89 pp.

A numerical method is described for solving the two-dimensional Navier-Stokes equations. Results for steady flow past a circular cylinder for Reynolds numbers up to 100, and past an elliptic cylinder for Reynolds numbers up to 200, are given.

MATHEMATICS RESEARCH CENTER, UNITED STATES ARMY
THE UNIVERSITY OF WISCONSIN

Contract No.: DA-31-124-ARO-D-462

NUMERICAL INTEGRATION OF THE NAVIER-STOKES EQUATIONS IN TWO DIMENSIONS

S. C. R. Dennis and Gau-Zu Chang

MRC Technical Summary Report #859
July 1969

Madison, Wisconsin